LAWRENCE
LIVERMORE
NATIONAL
LABORATORY

LLNL-TR-434300

Final Report - ITWG Round Robin #3

M. J. Kristo, R. K. Bibby, A. M. Gaffney, V. G. Genetti, J. Go, J. M. Gostic, P. M. Grant, R. A. Henderson, I. D. Hutcheon, G. L. Klunder, K. B. Knight, C. Koester, R. E. Lindvall, A. N. Martin, K. J. Moody, C. E. Ramon, E. C. Ramon, M. Robel, M. A. Sharp, M. J. Singleton, P. E. Spackman, L. T. Summers, R. W. Williams, P. T. Wooddy

June 7, 2010

Disclaimer

This work performed under the auspices of the U.S. Department of Energy by Lawrence Livermore National Laboratory under Contract DE-AC52-07NA27344.

LAWRENCE
LIVERMORE
NATIONAL
LABORATORY

LLNL-TR-XXXXXX

Final Report
Nuclear Smuggling International Technical Working Group (ITWG) Round Robin #3

Richard K. Bibby, Amy M. Gaffney, Victoria G. Genetti, Jackson Go, Julie M. Gostic, Patrick M. Grant, Roger A. Henderson, Ian D. Hutcheon, Gregory L. Klunder, Kimberly B. Knight, Carolyn Koester, Michael J. Kristo, Rachel E. Lindvall, Audrey N. Martin, Kenton J. Moody, Christina E. Ramon, Erick C. Ramon, Martin Robel, Frederick J. Ryerson, Michael A. Sharp, Michael J. Singleton, Paul E. Spackman, Leonard T. Summers, Ross W. Williams, Paul T. Wooddy

Lawrence Livermore National Laboratory

May 2010

Disclaimer

Auspices Statement

This work performed under the auspices of the U.S. Department of Energy by Lawrence Livermore National Laboratory under Contract DE-AC52-07NA27344.

Table of Contents

Tables

Figures

Laboratory:

Lawrence Livermore National Laboratory (United States of America)

Code Name:

Ural

Current Status:

Full nuclear forensics analysis of the two samples is complete. All uranium isotopic analyses indicate that both samples are weapons-usable, highly enriched uranium. Therefore, both seizures indicate that the statutes of the country of Texmex regarding the transport of uranium materials have been violated (>1 gram, >1% enriched in U235). Isotopic analysis by multicollector inductively coupled plasma-mass spectrometry (MC-ICP-MS) indicates that the two samples (Sample A, Sample B) have isotopic compositions that differ outside analytical uncertainty (k=2). The model ages of the two samples (apparent time since last chemical separation of parent and daughter nuclides) also differ outside analytical uncertainty (k=2). These results would indicate that, even with all of the other similarities between the two samples, the two questioned samples originate from different source materials.

Potential Issues:

None.

Delivery Details

Shipment arrived at LLNL Materials Management:	09:30 AM/February 17, 2010
Drum delivered to LLNL Nuclear Forensics Team:	11:30 AM/February 23, 2010
Package Opened/Exercise Started/Chain of Custody Initiated:	8:45 AM/February 26, 2010

Sample Identification

Sample B (Container: 3C19VLL6D7) is identified in LLNL's chain-of-custody records as "FSC-10-1-1."
Sample A (Container: 3C19VLLVDJ) is identified in LLNL's chain of custody records as "FSC-10-1-2."

Initial Inspection and Photo Documentation

Both samples 10-1-1 and 10-1-2 were solid, pin-shaped samples. They were both nominally 3 mm in thickness and 18 mm long. They were roughly trapezoidal in cross-section. Sample B (10-01-01) was approximately 6 mm at one end and 4 mm at the other end of the trapezoid, while Sample A (10-01-02) was approximately 5 mm at one end and 3 mm at the other end of the trapezoid. All surfaces appeared to have a slightly oxidized surface and otherwise appeared to be unfinished. In addition to standard photo documentation, we also took initial photomicrographs for each sample. During this evaluation, we noticed that each sample had the number "16" or "91" written by hand in what appeared to be a "Sharpie" type marker on both of their long, thin sides (~3 mm x 18 mm).

Figure 1. Shipping drum as received.

Figure 2. Material packaging

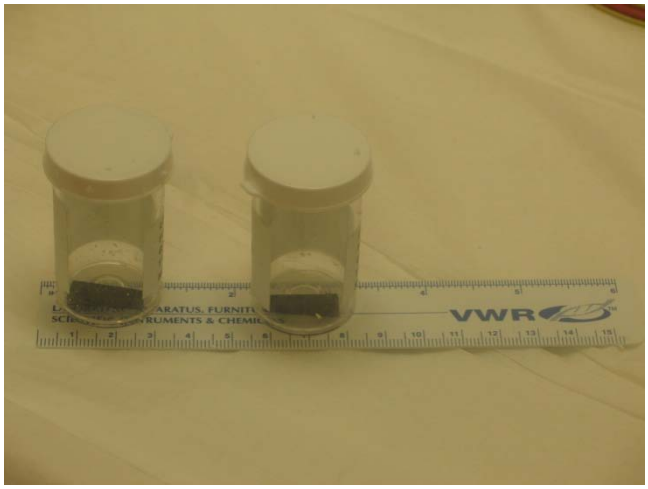

Figure 3. Two sample bottles
Left: Sample B (10-1-1)
Right: Sample A (10-1-2)

Sample Mass

Sample A	10-1-2	5.0640±0.0002 grams
Sample B	10-1-1	5.6196±0.0002grams

More rigorous measurement of sample dimensions

The samples were placed on 10X10 inch graph paper with a label identifying the sample and photographed using a D50 Nikon camera. Pictures were taken of each sample from one side and perspective. Both pieces are isosceles trapezoids and the angle between the long edges is 6 degrees. It would take 60 identical pieces of each to make flat washers with an inner radius of about 41 mm for the larger piece (Sample B), and an inner radius of about 32 mm for the smaller piece (Sample A). Annular castings are a typical geometry for storage of HEU. However, these calculated dimensions are not consistent with the cross-sectional dimensions of the standard 161 storage configuration of Y-12 (outer diameter of 12.700 cm, an inner diameter of 8.890 cm).

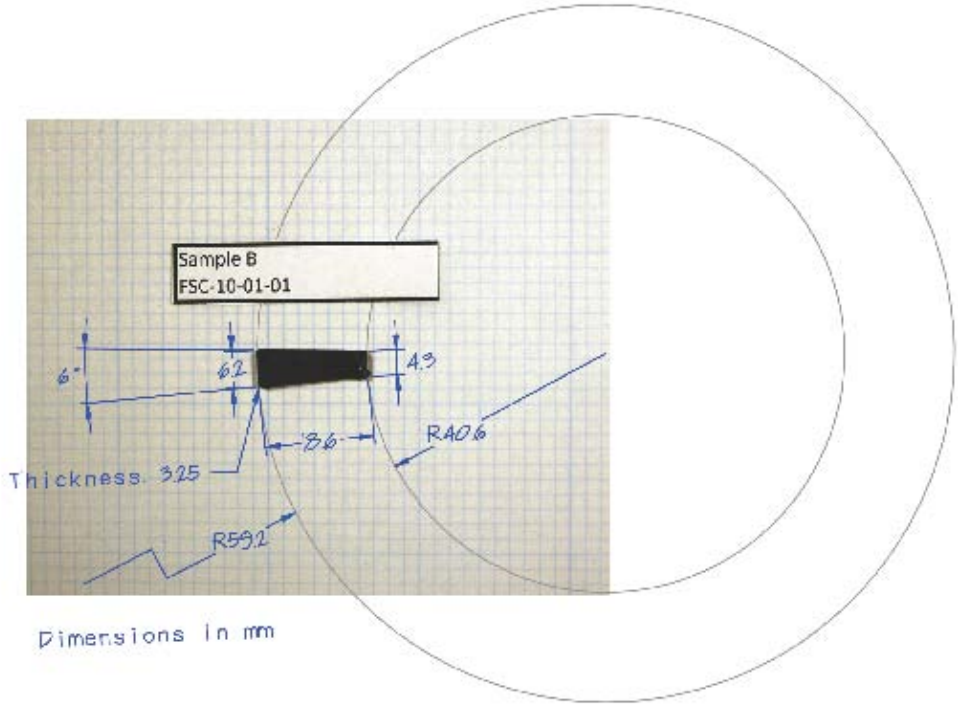

Figure 4. Dimensions of Sample B

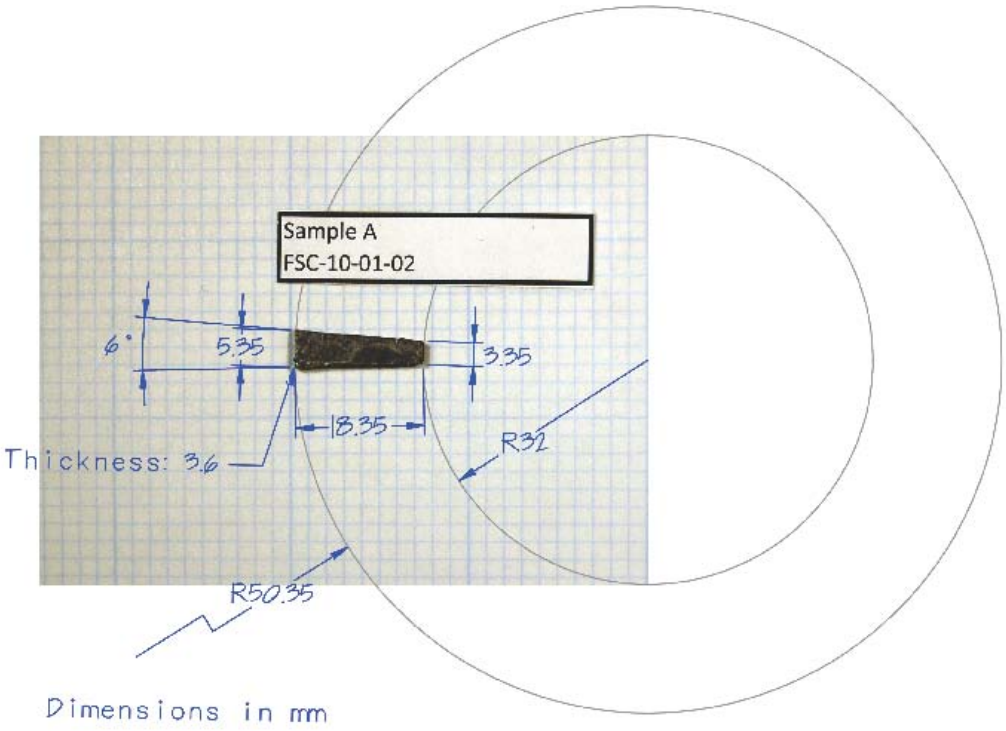

Figure 5. Dimensions of Sample A

Whole Sample Gamma Spectrometry Results

Note: Whole Sample Gamma Spectrometry was performed for initial categorization only. Higher accuracy and precision were obtained from whole solution gamma spectrometry and inductively coupled plasma/mass spectrometry.

Table 1. Whole Sample Gamma Spectrometry Results

ITWG exercise, 2/28/10, samples 100226

Results of 1-hour gamma-spec at 29 cm

	FSC-10-1-1		FSC-10-1-2	
grams 235U*	5.00	2.10%	4.65	2.30%
atom ratios				
232U/235U**	1.58E-10	6.30%	1.22E-10	8.60%
233U/235U	< 1.0e-4		<1.3e-4	
234U/235U	3.37E-03	16%	2.39E-03	24%
238U/235U	5.82E-02	26%	5.72E-02	33%
237Np/235U $	4.17E-06 $	9%	4.58E-06	10.70%
231Pa/235U	< 1.2e-7		< 1.3e-7	
239Pu/235U	< 5e-5		< 1.1e-4	

error bars are 1-sigma

* attentuation correction looks solid, but I'd treat these values with caution

**assumes aged material where 228Th is in equilibrium with 232U

$ bkg subtraction in limited area of spectrum was not great, value might increase by 5-10%

Analysis of samples by vis-NIR Reflectance Spectroscopy

Near-infrared (NIR) reflectance spectroscopy is a non-contact, nondestructive analytical technique that can provide chemical information on samples without prior sample preparation. The NIR spectral range, 1000- 2500 nm (4000 – 10000 cm^{-1}), primarily measures CH, OH, and NH vibrational overtones. Post-acquisition pattern-recognition algorithms can be applied to the data to allow direct comparisons or to search spectral libraries to determine the most appropriate match. We used a visible/NIR spectrometer (Analytical Spectral Devices, Inc.) equipped with three separate detectors to span the spectral regions from 350 -1000 nm, 1000 – 1800 nm, and 1800 – 2500 nm. A bifurcated, fiber-optic bundle transmitted light to the sample surface and collected reflected light to return to the spectrometer. The experimental apparatus is shown in Figure 6.

Each spectrum consisted of an average of 10 scans over the complete range of the spectrometer (350 – 2500 nm). Five spectral analyses of each sample were performed, with each analysis interrogating a different surface location on the same specimen. Data analysis was performed with the PLSplus/IQ add-on to the GRAMS/AI, v.8.00 software (ThermoGalactic), and discriminant analysis with mean-centering preprocessing was performed for statistical comparison of the data. The wavelength range from 350 – 2200 nm was adopted for evaluation, with the exception of the two regions where detector-switching induced large step-functions of signal intensity. The standoff height from the end of the fiber-optic to the surface of a sample was approximately 1 mm, with a resultant 5-mm spot size. A Kimwipe paper tissue was used as the reference specimen for all spectral measurements.

Reflectance spectra from the two samples (10-1-1 & 10-1-2) are shown in Figure 7, with each plot the average of the spectra collected at the five different sampling locations. Several notable features of these spectra were the high reflectance values, sloping baseline, detector shifts, and absorbance peaks. The surfaces of the each sample were more reflective than the reference standard (the Kimwipe tissue), resulting in the somewhat unusual situation of reflectance values > 1. In addition, the specular nature of the samples also contributed to the wavelength dependence, as manifest by the sloping baselines of the spectra. The specific detectors in the NIR spectrometer resulted in spectral discontinuities at 1000 and 1800 nm. For the two samples, the wavelength data in the first two spectral regions (350-1000 and 1000-1800 nm) were virtually identical, and discriminant analysis was unable to distinguish between 10-1-1 and 10-1-2. The third spectral region (>1800 nm) gave analogous results, but was bounded at 2200 nm due to absorbance effects of the fiber optics above that wavelength.

The measured spectral features in the NIR coincided with the absorption bands of the cellulose in the Kimwipe reference. Thus, in this experiment, these features could not be attributed to the surface chemical compositions of the samples. However, as the reference was consistent for both questioned samples, the comparative evaluation of 10-1-1 and 10-1-2 remained valid. Spectral comparisons of the two samples were performed in the visible and the near-infrared wavelength regions. The results of both visual and statistical (discriminant analysis) assessments of the data indicated that, considering only the surficial spectral features, both samples were quite similar in nature and were consistent with having derived from a common source.

Figure 6. Measurement configuration of vis-NIR spectrometer and fiber-optic probe.

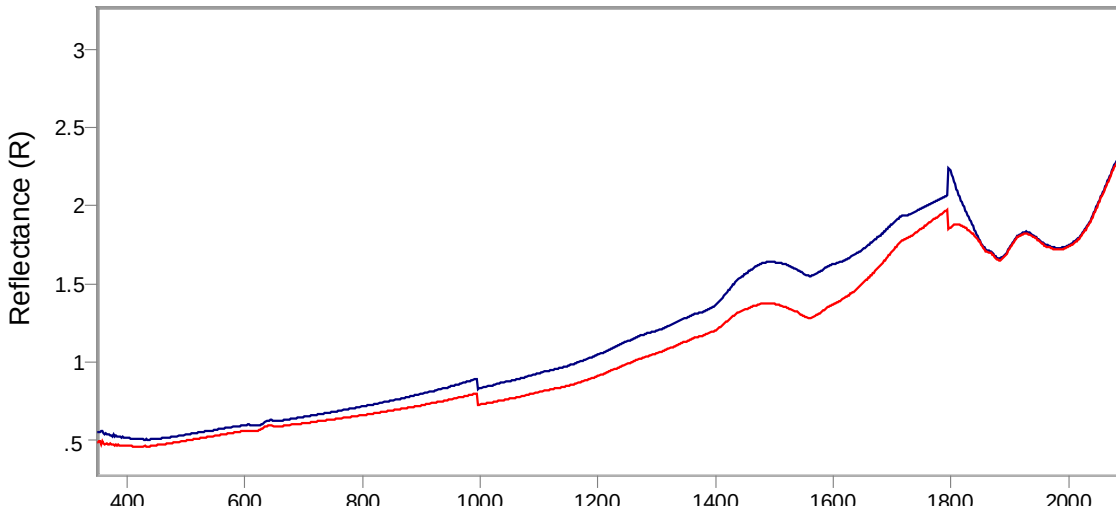

Figure 7. Reflectance spectra measured from the surfaces of the two ITWG RR3 specimens.

Organic analysis of samples by solid-phase microextraction (SPME) & gas chromatography-mass spectrometry (GC/MS)

Organic species associated with FSC #10-1-1 and FSC #10-1-2 were collected via solid-phase microextraction (SPME) and subsequently analyzed by gas chromatography/mass spectrometry (GC/MS). Volatile and semivolatile compounds in the questioned specimens were sampled using a 65-µm PDMS/DVB SPME fiber. This fiber type has proven useful for the collection of a variety of organic analytes. Individual samples were equilibrated in a 20-ml, Teflon-lined and septum-sealed, glass vial at 55ºC for 15 minutes prior to performing a 30-minute SPME collection of analytes in the vial headspace. After sample exposure, the SPME fibers were desorbed for 1 minute at 250ºC and analyzed by GC/MS. The GC column employed was a 30-m, DB-5ms column with 0.25-mm i.d. and 0.25-µm film thickness. The temperature of the GC oven was programmed as follows: 30ºC for 3 minutes, ramped at 8ºC/min to 300ºC, and maintained at 300ºC for 3 minutes. The MS was scanned from *m/z* = 29-550 amu. An unused 20-ml, Teflon-lined and septum-sealed, glass vial was similarly analyzed to provide a method blank. Organic components in each sample were tentatively identified using AMDIS (Automated Mass Spectral Deconvolution and Identification System, ver. 2.62, March 2005) and the NIST Mass-Spectral Library (2005).

Many different compounds were present in the headspace of each of the questioned specimens. As the samples were metal specimens, rather than porous material, the analyses predominantly interrogated analytes sorbed on the surfaces. The total-ion chromatograms (TICs) produced by the two samples were similar in appearance, suggesting that they shared common attributes (e.g., a common source or common environmental conditions resulting from processing, packaging, transport, contamination, etc., or both). Such assessment can be initially performed via visual examination of the TICs produced by the samples (see Figure 8). Inspection of TICs generated under identical analysis conditions allows a quick (but subjective and conservative) comparison of both the relative numbers and the relative concentrations of detected compounds.

In addition to visual inspection of the TICs, the AMDIS software was used to tentatively identify the multiplicity of species detected in the samples. While AMDIS successfully deconvolutes overlapping spectra, we have found that it often incorrectly reports the presence of several components when only a single compound is present, and it often fails to properly identify alkanes because of the very similar spectral features of these compounds. Despite its limitations, however, proper use of AMDIS is a valuable analytic tool that can provide a common protocol for GC/MS data reduction among independent laboratories.

After blank subtraction, the chemical species present in the samples in greatest abundance, and tentatively identified based on the comparison of their spectra with those contained in the NIST library, are given in Table 2. In the opinion of experienced mass spectroscopists, the similarities of the total-ion chromatograms produced by SPME-GC/MS from samples 10-1-1 and 10-1-2 were consistent with their surficial analytes having originated from a common source, and/or by the exposure of the samples to similar environments. The GC/MS analyses were qualitative runs. Nevertheless, because of the identical experimental conditions, rigorous statistical analysis of the similarity between the two specimens could be performed via the nonparametric Spearman Correlation Coefficient. Using empirical analytes common to the samples, and their relative peak areas, the Spearman ρ was computed to be 0.88 ($n = 28$). [Similar (and related) to the Pearson coefficient, $\rho = 1$ indicates a perfect correlation, while $\rho = 0$ signifies no correlation.] Thus, the Spearman $\rho = 0.88$ specifies a strong correlation between 10-1-1 and 10-1-2, at least with respect to the volatile/semivolatile species sorbed on their surfaces. Such "route" correlation may well be independent of any "source" trending, however.

Several of the compounds detected in 10-1-1 and 10-1-2 are products whose general uses are known. For example, benzaldehyde, acetophenone, and nonanal are common fragrance compounds used in perfumes. Acetophenone is also used as a catalyst for olefin polymerization and as a photosensitizer in organic synthesis. 2-ethyl-1-hexanol is regularly used for mercerizing textiles, or as a dye or resin solvent, and it possesses some antifoaming properties. 3-methylheptyl acetate has been identified by the U.S. FDA as a compound found in PVC; and 3,3-dimethyl hexane is listed as a component of gasoline by the U.S. OSHA. Finally, 2-ethylhexyl salicylate is a common solvent used in making solid sunscreens, as it absorbs UV light.

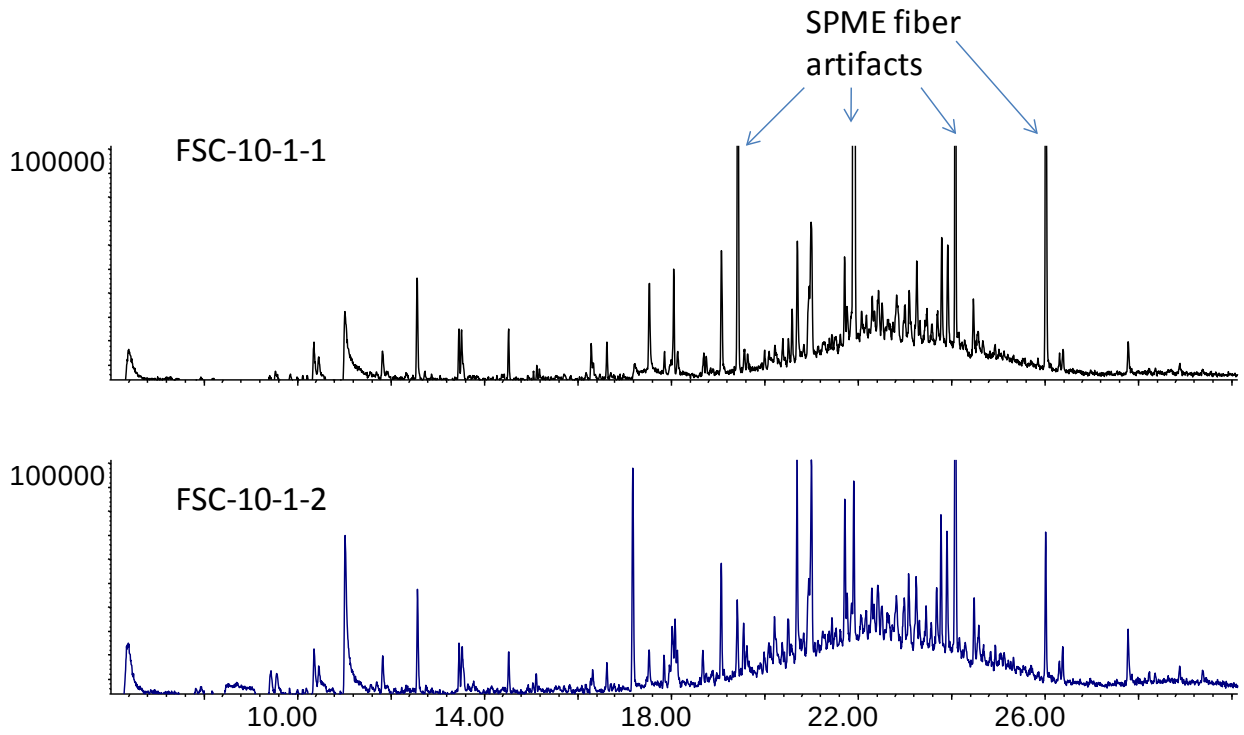

Figure 8. Total-ion chromatograms produced by SPME-GC/MS analyses of FSC #10-1-1 and FSC #10-1-2 (no blank subtractions).

Table 2. Organic analytes present on ITWG RR 3 questioned specimens, with AMDIS figures-of-merit (purity & weight) for compound identification also given.

Tentative ID	t_R (min)	Purity/Weight (%)	FSC 10-1-1	FSC 10-1-2
2,2-dimethylpropanoic anhydride	7.84	41/76	*	*
ethyl 2-((methylamino)carbonyl)hydrazine carboxylate	7.94	12/66	*	X
unknown (broad peak)	8.68	nd		X
2-ethyl hexanal	9.4	52/73	*	X
benzaldahyde	9.55	82/89	*	X
unknown	10.47	50/-	X	X
2-ethyl-1-hexanol	11.02	91/93	X	X
acetophenone	11.84	70/85	X	X
nonanal	12.57	87/84	X	X
3-methylheptyl acetate	13.46	86/95	X	X
unknown	14.52	27/-	X	X
unknown	15.12	40/-	*	*
unknown	16.33	38/-	*	X
2,4-diisocyanato benzene	17.19	89/92		X
unknown	17.53	43/-	X	X
3,3-dimethyl hexane	17.97	37/71		X
unknown	18.01	14/-		X
1,3-dihydro-5-methyl-2H-benzimidazol-2-one	18.09	69/79		X
unknown	18.14	25/-	X	X
bis(2-ethylhexyl) ester oxalic acid	19.56	62/82	*	X
1-tert-butoxy-2-ethoxyethane	20.71	71/73	X	X
2-methyl pentadecane	21.02	48/63	X	X
3-ethyl-3-methyl hexane	21.73	61/79	X	X
4,4-dimethyl undecane	23.1	44/82	X	X
cis-1,1'-(1,2-cyclobutanediyl)bis-benzene	23.25	40/91	X	X
2-methylundecane	23.78	66/81	X	X
2-ethylhexyl salicylate	23.91	53/88	X	X
3-ethyl-3-methyl hexane	24.47	58/80	X	X
bis(dimethylamino)trifluorophosphorane	24.58	12/71	X	X
unknown	24.93	17/-	*	X
3,4-dihydro-4-phenyl-1(2H)naphthalenone	26.38	43/67	X	X
unkonwn	28.89	13/-	*	*
unknown	29.4	4.1/-	*	*

X if peak area >20,000 counts

* if peak area <20,000 counts

.

Stereo microscopy

The exterior of samples A and B were fully documented by optical microscopy. Images were acquired as follows: the series goes from the wide end of the sample to the narrow end. When the depth of field did not allow all portions of the image to be in focus, the focus was adjusted and two images were taken of the same area. For the flat side where the samples were too wide for the field, the series first goes from top to bottom, then back to the top and stepping to the right. The samples were turned counter-clockwise looking down the axis from the wide end to the narrow. Due to the limited working distance of the optical microscope, we were unable to photograph the ends of each piece until after sample aliquoting (sectioning of the intact samples).

The exterior of both samples were quite similar, although Sample A (FSC 10-1-2) appeared to have a greater number of surface "decorations" (obvious features, perhaps inclusions or occlusions, of different composition than the bulk material). For both samples, the dominant feature of the two large flat surfaces was a series fairly regular grooves or striations (~ 15/mm), perhaps machining marks either on the piece itself or from the metal mold. The long, narrow sides of both pieces also showed striations, but more irregular and widely spaced, perhaps due to machining. In Figure 17, we see clear evidence of a rough sawing or chiseling on one of the edges of Sample A (FSC 10-1-2). Both ends of each piece do not appear to have striations, but show a uniform, oxidized appearance, perhaps these surfaces are as-cast.

Note the number "16" or "91" in Figure 15; the number was written on both long edges of both samples, although in different orientations.

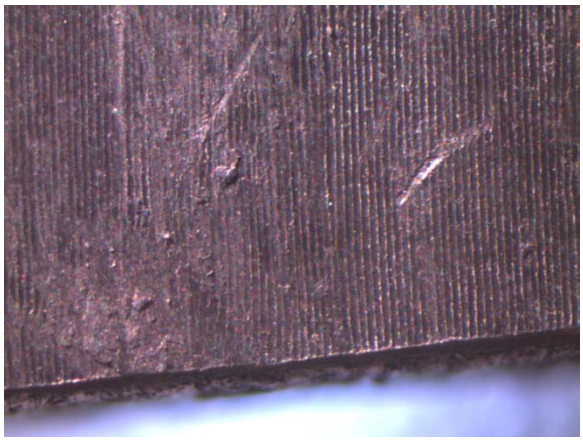

Figure 9. Flat side of Sample B (FSC 10-1-1)

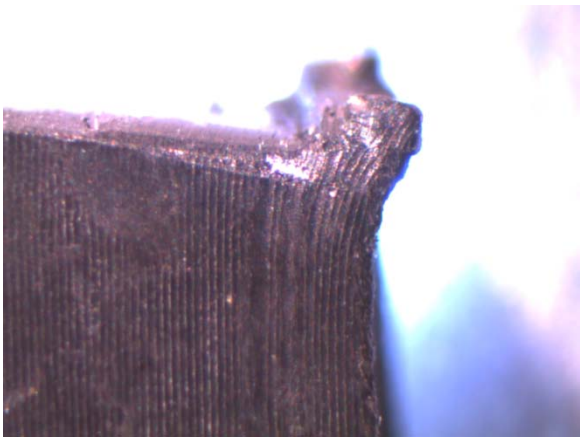

Figure 10. Burr on Sample B (FSC 10-1-1)

Figure 11. Edge of Sample B (FSC 10-1-1)

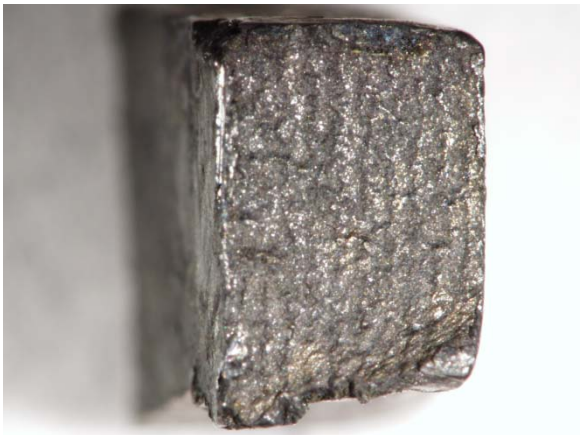

Figure 12. End of Sample B(FSC 10-1-1)

Figure 13. Other end of Sample B (FSC 10-1-1)

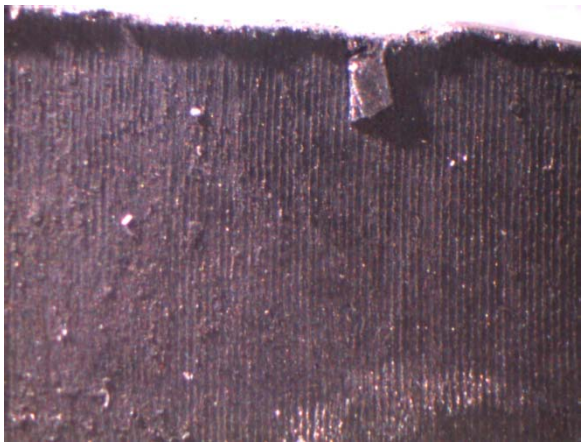

Figure 14. Flat side of Sample A (FSC 10-1-2)

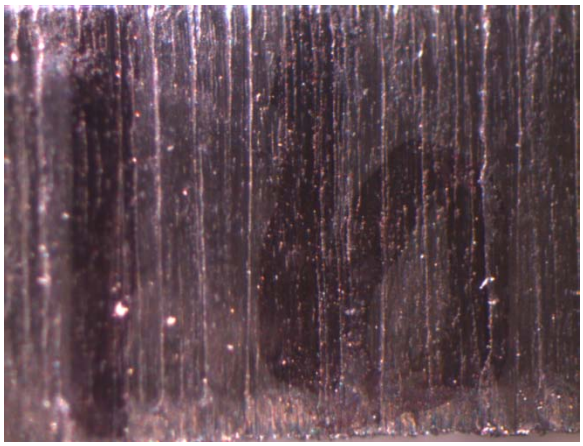

Figure 15. Edge of Sample A (FSC 10-1-2)

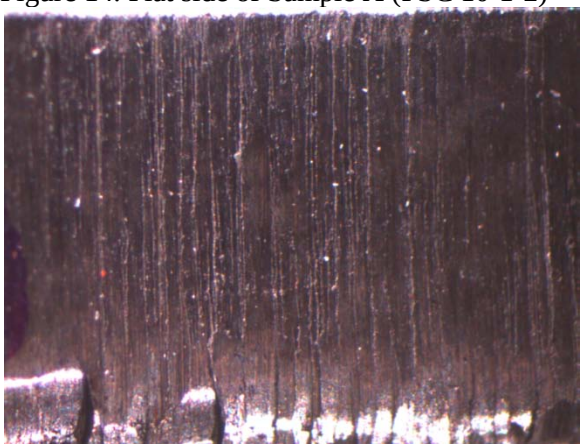

Figure 16. Edge of Sample A (FSC 10-1-2)

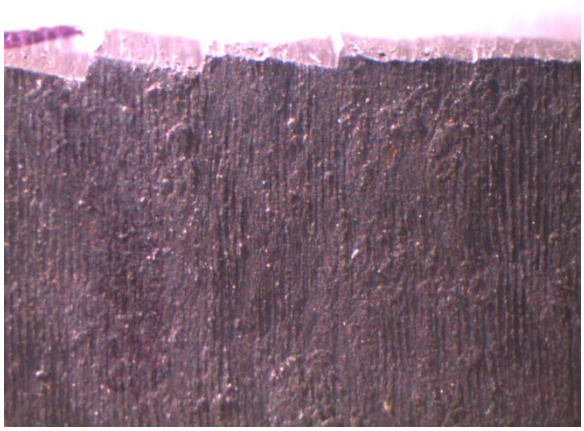

Figure 17. Rough-cut edge of Sample A (FSC 10-1-2)

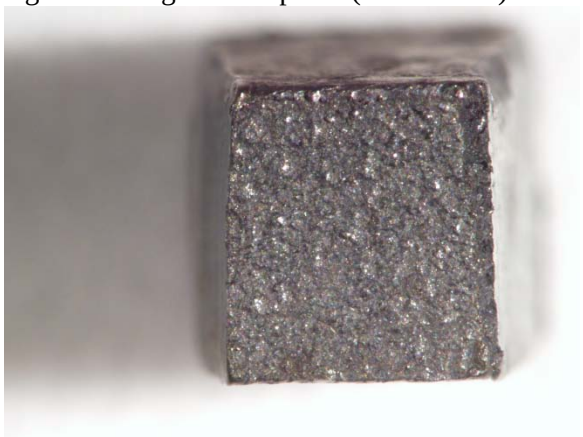

Figure 18. End of Sample A (FSC 10-1-2)

Figure 19. Other end of Sample A (FSC 10-1-2)

Figure 20. Orange & blue “decorations”

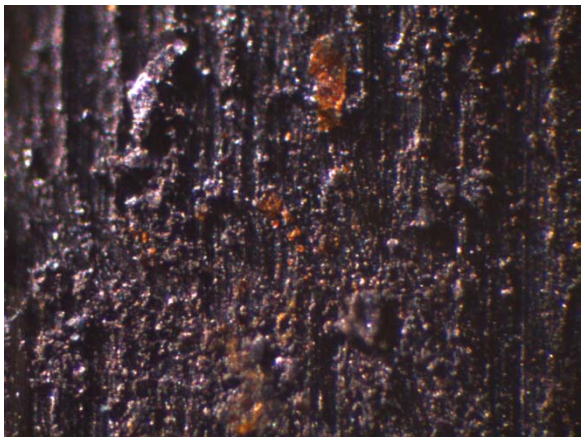

Figure 21. Close-up of orange “decoration”

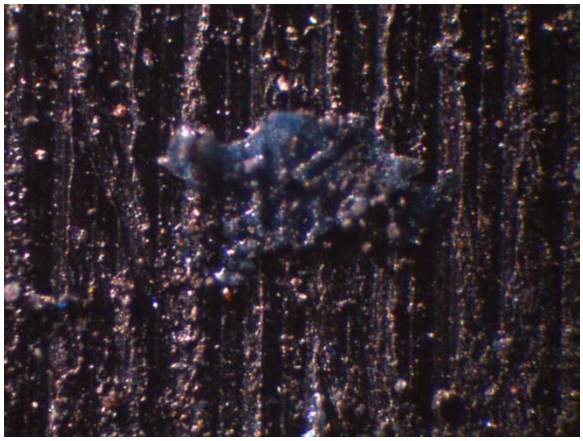

Figure 22. Close-up of blue “decoration”

Scanning electron microscopy (SEM)/ X-ray energy dispersive spectrometry (EDS)

Several “interesting” features were found during optical microscopy, so SEM was used to investigate the nature of the observed features. Once in the SEM, though, it was agreed that a more thorough effort to document all 6 surfaces for each of the two samples was prudent. Images were taken with overlap at 100x for each of the six surfaces using the secondary electron detector on an FEI INSPECT- F FE-SEM. The SEM was operated at a constant 15kv and spot size 6. On occasion, images were also taken with the backscatter detector to document the compositional variation of the materials observed on the surface. At least one (often three) areas of interest were identified on each of the sides and higher resolution images and an EDS spectrum were collected for documentation.

In general, evidence for mechanical markings is clearly visible on all four of the long sides of the samples with no evidence on the ends of similar markings. Several impurities were identified appearing to be both in and on the metal rod. The compositions of those interrogated consisted of Fe rich, Al rich, C rich, and more complex compositions that included Ti, Na, Cl as well. One particle which emitted few xrays was also found and might be Be.

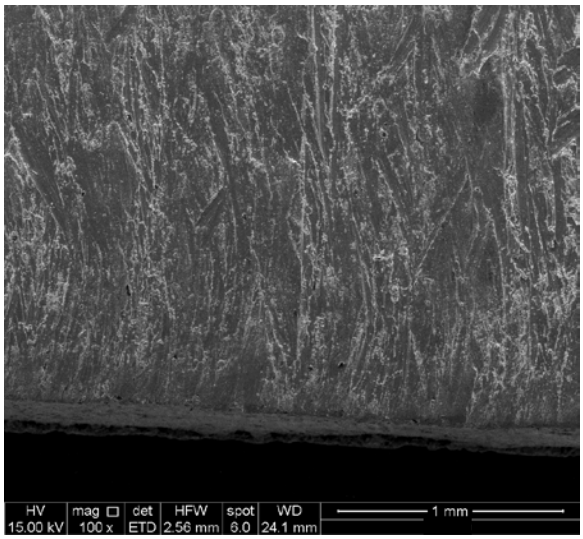

Figure 23. Edge of Sample B (FSC-10-1-1)

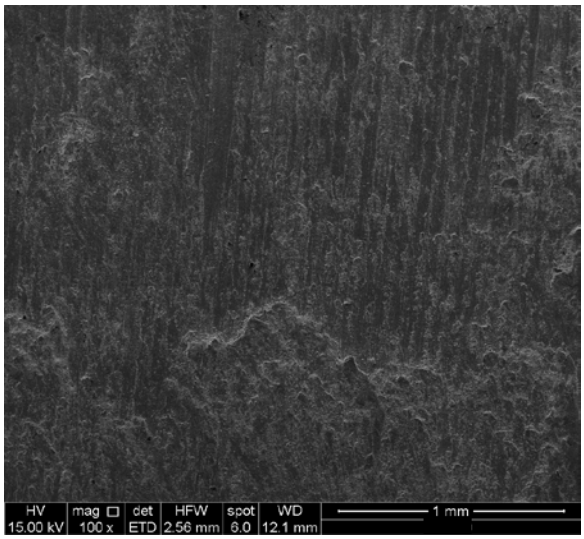

Figure 24. Flat surface of Sample B (FSC-10-1-1)

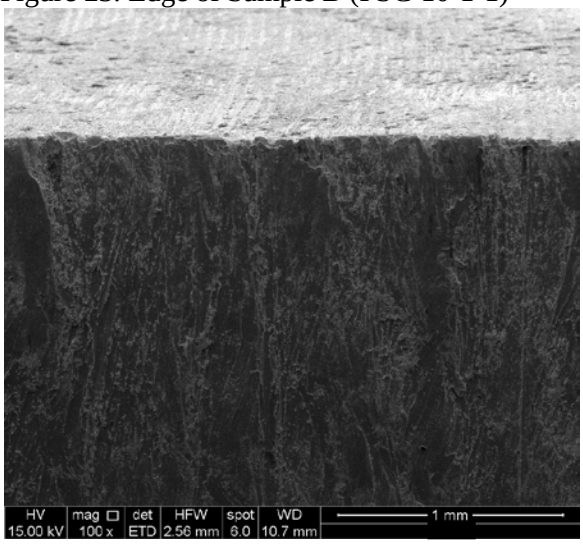

Figure 25. Edge/Flat of Sample B (FSC-10-1-1)

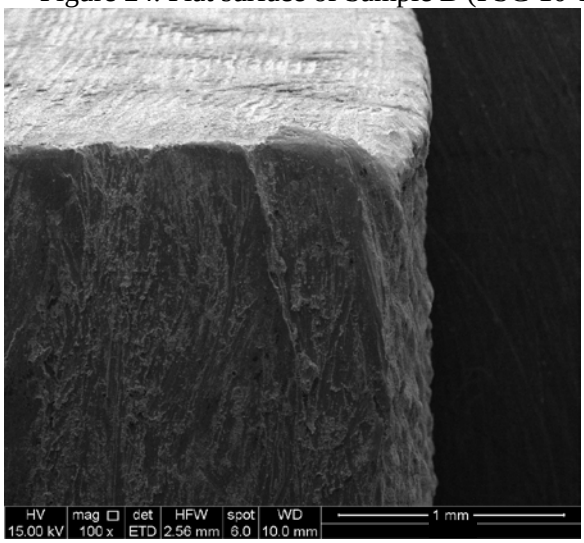

Figure 26. Corner of Sample B (FSC-10-1-1)

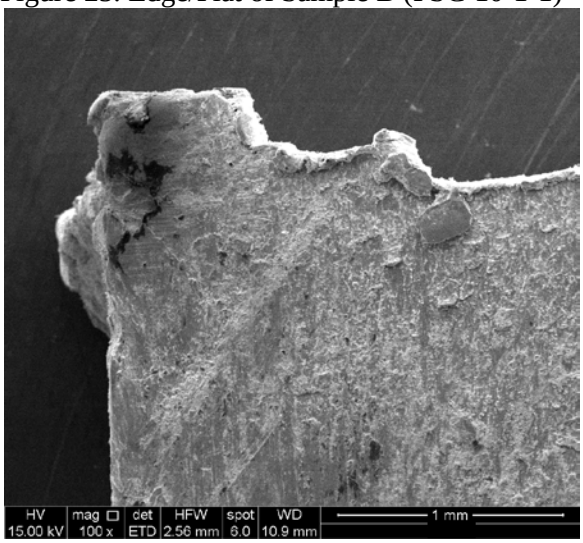

Figure 27. Burr on Sample B (FSC-10-1-1)

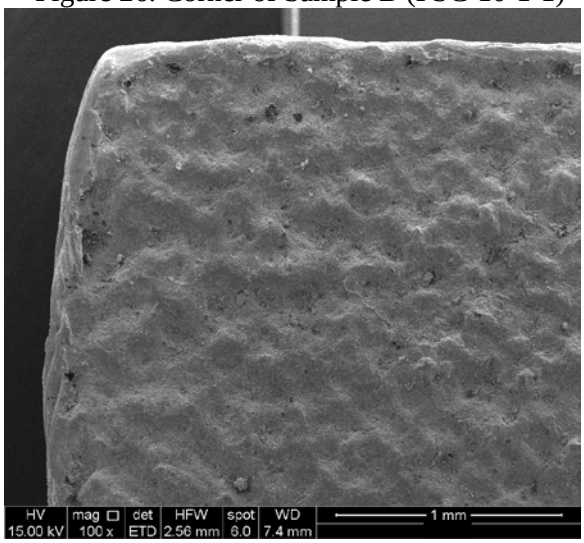

Figure 28. End of Sample B (FSC-10-1-1)

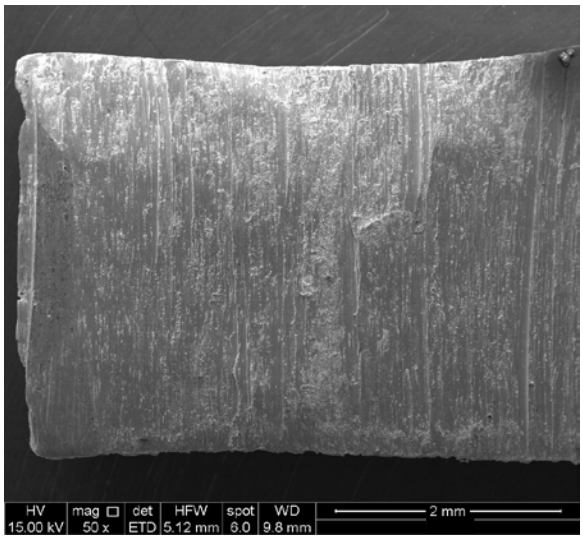

Figure 29. Edge of Sample A (FSC-10-1-2)

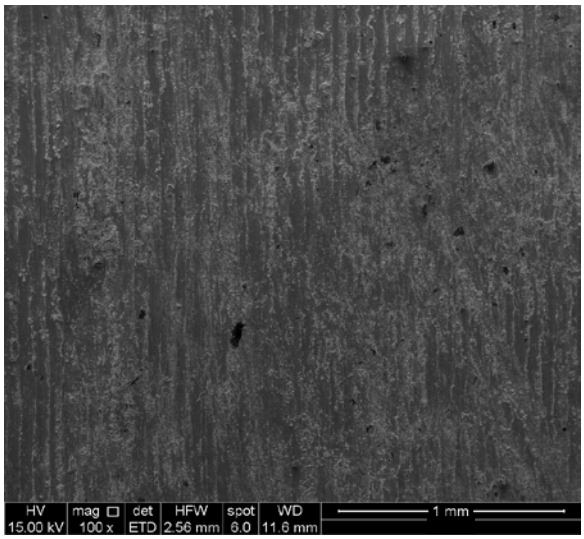

Figure 30. Flat side of Sample A (FSC-10-1-2)

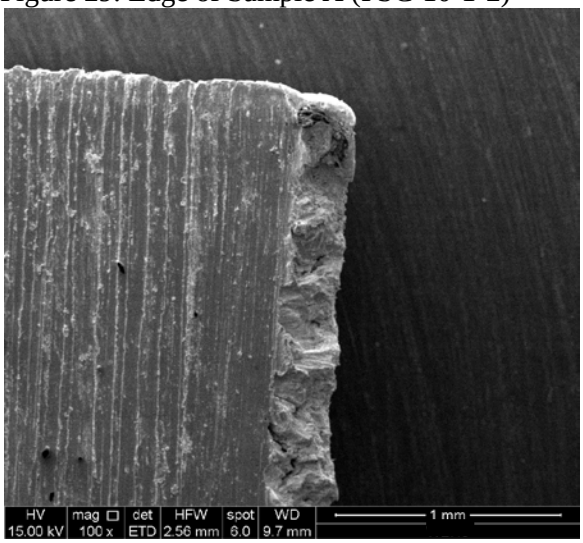

Figure 31. End of Sample A (FSC-10-1-2)

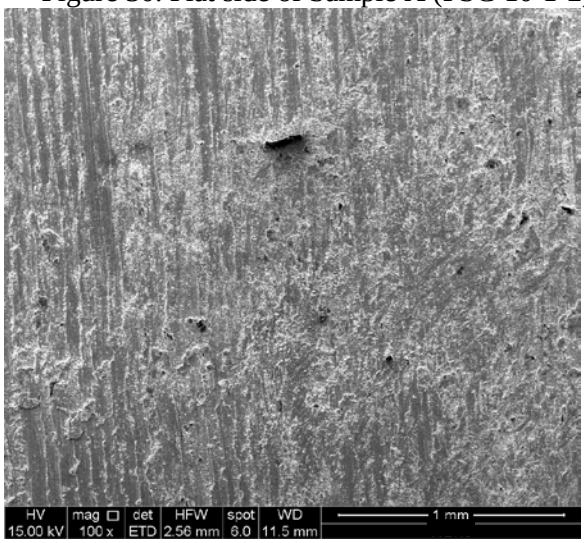

Figure 32. Flat side of Sample A(FSC-10-1-2)

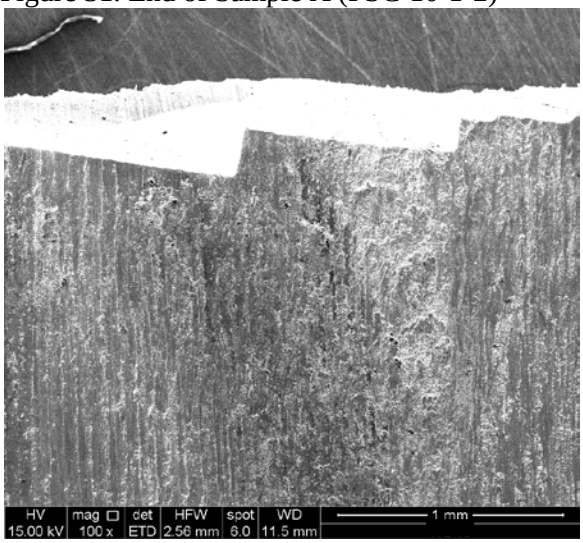

Figure 33. Rough edge of Sample A (FSC-10-1-2)

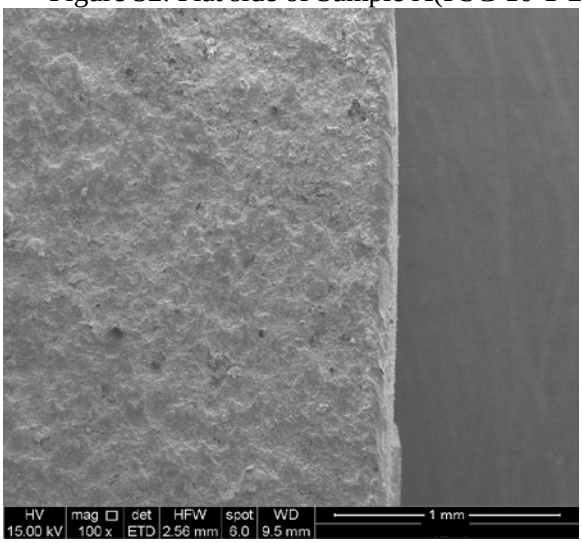

Figure 34. End of Sample A (FSC-10-1-2)

Aliquoting of each sample into 4 sub-samples (A, B, C, D)

Samples were cut on an ISOMET 2000 wet saw. A separate 6-inch diameter diamond wafering blade was used for each sample. Cutting commenced with sample 10-1-1. The narrow end of the bar was clamped to the saw arm and the first cut was made approximately 4mm from edge of the wide end and produced sample 10-1-1-D. The following piece was cut 4mm from the previous cut and produced sample 10-1-1-C. The last cut was made such that the two final pieces were approximately the same size where the clamped metal was 10-1-1-A and the piece cut off was 10-1-1-B.

The next sample was also clamped on the narrow side but this time the cut was made 4.5mm from the edge of the wide side. That cut produced sample 10-1-2-D. The next cut was made 4.5 mm from the previous cut and produced sample 10-1-2-C. The next cut was made 4mm from the previous cut and produced sample 10-1-2-B with the remaining piece still clamped on the saw arm as 10-1-2-A.

At first, the saw was operated at 100 rpm with the weight set to 250 grams. However, we slowly increased first the weight then the speed of the saw so that the cutting would proceed more quickly. The final settings for the sawing (300rpm and 500 weight) were used slightly before half way through the first cut and were maintained for the remaining cuts. The cuts under these conditions took about 10 minutes each. As each piece was cut it was placed in a pre-labeled centrifuge tube to air dry. Once all the cuts were completed, each of the centrifuge tubes was filled with approximately 4ml of acetone, shaken, and the acetone and sample were poured out onto a cotton swipe. Weights were then taken and recorded after the acetone had dried (as determined by weight stability).

A saw blank was provided which consisted of a piece of ceramic conditioning stick that had been cut seven times with each of the two blades used in the operation. The ceramic material was put into the same type of centrifuge tube as the samples and processed with acetone as described above. A radchem blank and a mass spec blank were prepared by taking a centrifuge tube, filling it with acetone, and pouring it out before capping the tube.

Samples 10-1-1-B and 10-1-2-C were designated for MS while 10-1-1-C and 10-1-2-B were set aside for radiochemistry. SEM was then used to image the freshly cut side of sections A and D. The imaging was done as described above except that the map was prepared both with both backscattered and secondary electron signals.

Isotopic analysis by inductively coupled plasma-mass spectrometry (ICP-MS)

Sub-sample B for sample B (FSC-10-1-1) and sub-sample C for sample A (FSC-10-1-2) were dissolved, relevant elemental fractions were separated and purified, and the resulting solutions analyzed by multicollector inductively coupled plasma-mass spectrometry (MC-ICP-MS) using a NuPlasma HR. Uranium Isotopic results are listed in Table 3. Plutonium Isotopic results are listed in Table 4. Neptunium concentrations are listed in Table 5.

"Model Ages" as determined by MC-ICP-MS are shown in Table 6 ($^{234}U \rightarrow ^{230}Th$ system), Table 7 ($^{241}Pu \rightarrow ^{241}Am$ system), and Table 8 ($^{235}U \rightarrow ^{231}Pa$ system). These model ages estimate the time since last chemical purification of the parent nuclide from the daughter nuclide (assuming complete purification). Incomplete purification will produce ages that are greater than the true time of the last chemical purification, and fractionation of daughter from parent nuclide during subsequent processing will result in ages that are either greater or less than the true time of purification, depending on the sense of fractionation.

Table 9 gives the uranium assay measurements by isotope dilution mass spectrometry (IDMS), both by isotope and for total elemental uranium.

Table 3. Uranium isotopic composition from MC-ICP-MS

		Atom Percent									
ITWG Sample ID	FSC Sample ID	233U	Expanded Uncert. (k=2)	234U	Expanded Uncert. (k=2)	235U	Expanded Uncert. (k=2)	236U	Expanded Uncert. (k=2)	238U	Expanded Uncert. (k=2)
Sample A	FSC-10-1-2	0.0000329	0.0000044	1.00370	0.00040	92.9832	0.0085	0.38597	0.00056	5.6271	0.0061
Sample B	FSC-10-1-1	0.0000431	0.0000044	0.97768	0.00041	91.5078	0.0094	0.40618	0.00059	7.1083	0.0077

		Atomic Ratios							
ITWG Sample ID	FSC Sample ID	233U/235U	Expanded Uncert. (k=2)	234U/235U	Expanded Uncert. (k=2)	236U/235U	Expanded Uncert. (k=2)	238U/235U	Expanded Uncert. (k=2)
Sample A	FSC-10-1-2	0.000000354	0.000000048	0.0107944	0.0000043	0.0041510	0.0000060	0.060517	0.000066
Sample B	FSC-10-1-1	0.000000471	0.000000048	0.0106842	0.0000043	0.0044387	0.0000065	0.077680	0.000084

Table 4. Plutonium isotopic composition from MC-ICP-MS

		atomic ratios						ng/g U-metal	
ITWG Sample ID	FSC Sample ID	240Pu/239Pu	Expanded Uncertainty (k=2)	241Pu/239Pu	Expanded Uncertainty (k=2)	242Pu/239Pu	Expanded Uncertainty (k=2)	Total Pu	Expanded Uncertainty (k=2)
Sample A	FSC-10-1-2-C	0.06574	0.00045	0.000662	0.000013	0.001375	0.000038	7.04	0.24
Sample B	FSC-10-1-1-B	0.06238	0.00043	0.000556	0.000011	0.001086	0.000025	14.10	0.48
Analysis date for the Pu isotopes is 18-Mar-10									

Table 5. Neptunium concentrations from MC-ICP-MS

		atomic ratio		microgram/g U-metal	
ITWG Sample ID	FSC Sample ID	237Np/238U	std. uncert.	237Np	Expanded Uncertainty (k=2)
Sample A	FSC-10-1-2-C	0.00007801	0.00000136	4.41	0.15
Sample B	FSC-10-1-1-B	0.00004800	0.00000086	3.42	0.12
note that the 237Np concentration has units of ppm					
whereas the other concentrations are given in ppb.					

Table 6. Age-dating from MC-ICP-MS using the $^{234}U \rightarrow ^{230}Th$ System

		ng/g U-metal		atoms/g U-metal		atoms/g U-metal		atomic ratio	
ITWG Sample ID	FSC Sample ID	232Th		230Th	std. uncert.	234U	std. uncert.	230Th / 234U	std. uncert.
Sample A	FSC-10-1-2-C	< 1.6		4.962E+14	1.2E+12	2.5587E+19	3.5E+16	0.000019391	0.000000055
Sample B	FSC-10-1-1-B	< 1.4		4.254E+14	1.0E+12	2.4915E+19	3.4E+16	0.000017074	0.000000048
		years before							
		Reference Date	9-Mar-10						
ITWG Sample ID	FSC Sample ID	**Model Age (years)**	**Expanded Uncertainty (years)**	**Model Date**	**Expanded Uncertainty (days)**				
Sample A	FSC-10-1-2-C	6.861	0.041	29-Apr-03	15				
Sample B	FSC-10-1-1-B	6.041	0.036	22-Feb-04	13				

Table 7. Age-dating from MC-ICP-MS using the $^{241}Pu \rightarrow ^{241}Am$ System

		ng/g U-metal		atoms/g U-metal		atoms/g U-metal		atomic ratio	
ITWG Sample ID	FSC Sample ID	241Am	Expanded Uncertainty (k=2)	241Am	std. uncert.	241Pu	std. uncert.	41Am / 241Pu	std. uncert.
Sample A	FSC-10-1-2-C	0.004372	0.000028	1.0920E+10	5.4E+07	1.107E+10	1.7E+08	0.987	0.016
Sample B	FSC-10-1-1-B	0.009740	0.000061	2.433E+10	1.2E+08	1.868E+10	2.8E+08	1.303	0.020

		years before	
		Reference Dat	16-Mar-10

ITWG Sample ID	FSC Sample ID	**Model Age (years)**	**Expanded Uncertainty (years)**	**Model Date**	**Expanded Uncertainty (days)**
Sample A	FSC-10-1-2-C	14.35	0.33	8-Nov-95	121
Sample B	FSC-10-1-1-B	17.46	0.37	28-Sep-92	135

Table 8. Age-dating from MC-ICP-MS using the $^{235}U \rightarrow ^{231}Pa$ System

		atoms/g U-metal		atoms/g U-metal		atomic ratio	
ITWG Sample ID	FSC Sample ID	231Pa	std. uncert.	235U	std. uncert.	231Pa / 235U	std. uncert.
Sample A	FSC-10-1-2-C	7.870E+13	4.0E+11	2.3704E+21	3.2E+18	3.320E-08	1.8E-10
Sample B	FSC-10-1-1-B	8.212E+13	4.1E+11	2.3320E+21	3.2E+18	3.521E-08	1.8E-10

		years before	
		Reference Date	21-Mar-10

ITWG Sample ID	FSC Sample ID	**Model Age (years)**	**expanded uncert. (k=2)**	**Model Date**	**Expanded Uncertainty (days)**
Sample A	FSC-10-1-2-C	33.73	0.36	29-Jun-76	132
Sample B	FSC-10-1-1-B	35.77	0.37	14-Jun-74	136

Table 9. Uranium assay measurements using isotope dilution mass spectrometry

The assay, below, does not include the 232U results.

		g-isotope / g- U-metal					
	Sample ID	233U	std. uncert.	234U	std. uncert.	235U	std. uncert.
Sample A	FSC-10-1-2-C	3.25E-07	2.2E-08	9.944E-03	1.3E-05	9.252E-01	1.2E-03
Sample B	FSC-10-1-1-B	4.25E-07	2.2E-08	9.683E-03	1.3E-05	9.102E-01	1.2E-03

		g-isotope / g- U-metal					
	Sample ID	236U	std. uncert.	238U	std. uncert.		
Sample A	FSC-10-1-2-C	3.8567E-03	5.9E-06	5.6704E-02	8.2E-05		
Sample B	FSC-10-1-1-B	4.0572E-03	6.2E-06	7.161E-02	1.0E-04		

	Sample ID	Assay (g-uranium / g-metal)					
Sample A	FSC-10-1-2-C	U (g) / Metal (g)	Exp. Uncert. (k=2)				
Sample B	FSC-10-1-1-B	0.9957	0.0025				
		0.9955	0.0025				

Trace elemental impurities

An aliquot of the initial dissolution of the sub-samples B was analyzed by quadrupole inductively coupled plasma-mass spectrometry using a Thermo X-7 ICP-MS for trace impurity concentrations. The concentrations are listed in Table 10. We note the presence of Zr and Er, both of which can be used in the oxide form as mold coatings for uranium casting.

Table 10. Trace Elemental Impurities in Samples FSC-10-1-1 and FSC-10-1-2

Element	Units	FSC 10-1-1	uncertainity k=2	FSC 10-1-2	uncertainity k=2	Element	Units	FSC 10-1-1	uncertainity k=2	FSC 10-1-2	uncertainity k=2
Be	ug / g metal	< 0.006	---	< 0.03	---	Cd	ug / g metal	< 0.069	---	< 0.073	---
Na	ug / g metal	< 84	---	< 98	---	Sn	ug / g metal	< 0.178	---	< 0.16	---
Mg	ug / g metal	< 0.36	---	< 0.12	---	Sb	ug / g metal	< 0.036	---	< 0.024	---
Al	ug / g metal	27	6	23	7	Cs	ug / g metal	< 0.031	---	< 0.032	---
K	ug / g metal	< 6	---	< 3.9	---	Ba	ug / g metal	< 0.054	---	< 0.054	---
Ca	ug / g metal	< 2.7	---	< 2.7	---	La	ug / g metal	< 0.012	---	< 0.012	---
Ti	ug / g metal	< 3.8	---	< 3.9	---	Ce	ug / g metal	< 0.0024	---	< 0.0024	---
V	ug / g metal	1.2	0.6	1.0	0.6	Pr	ug / g metal	< 0.0024	---	< 0.0024	---
Cr	ug / g metal	23	3	21	3	Nd	ug / g metal	< 0.009	---	< 0.012	---
Mn	ug / g metal	9.2	0.9	8	1	Sm	ug / g metal	< 0.015	---	< 0.009	---
Fe	ug / g metal	99	6	88	4	Eu	ug / g metal	< 0.0048	---	< 0.003	---
Co	ug / g metal	1.0	0.2	1.0	0.2	Gd	ug / g metal	< 0.006	---	< 0.009	---
Ni	ug / g metal	61	3	66	4	Tb	ug / g metal	< 0.0024	---	< 0.006	---
Cu	ug / g metal	13	1	13	2	Dy	ug / g metal	< 0.012	---	< 0.003	---
Zn	ug / g metal	< 0.12	---	< 0.15	---	Ho	ug / g metal	< 0.0024	---	< 0.003	---
Ga	ug / g metal	< 0.06	---	< 0.06	---	Er	ug / g metal	0.45	0.04	0.22	0.03
Ge	ug / g metal	< 0.27	---	< 0.15	---	Tm	ug / g metal	< 0.006	---	< 0.006	---
As	ug / g metal	< 0.21	---	< 0.15	---	Yb	ug / g metal	< 0.006	---	< 0.009	---
Se	ug / g metal	< 0.09	---	< 0.21	---	Lu	ug / g metal	< 0.0024	---	< 0.003	---
Rb	ug / g metal	< 0.029	---	< 0.033	---	Hf	ug / g metal	< 0.052	---	< 0.034	---
Sr	ug / g metal	< 0.009	---	< 0.012	---	Ta	ug / g metal	0.594	---	0.37	---
Y	ug / g metal	< 0.0024	---	< 0.006	---	W	ug / g metal	34.7	0.5	34.2	0.6
Zr	ug / g metal	10.5	0.5	5.8	0.4	Re	ug / g metal	1.2	0.1	17.5	0.8
Nb	ug / g metal	< 0.057	---	< 0.086	---	Ir	ug / g metal	0.35	0.03	0.17	0.02
Mo	ug / g metal	51	1	51	2	Pt	ug / g metal	0.4	0.1	0.4	0.1
Ru	ug / g metal	< 0.027	---	< 0.033	---	Tl	ug / g metal	< 0.015	---	< 0.012	---
Rh	ug / g metal	< 0.052	---	< 0.047	---	Pb	ug / g metal	< 0.037	---	< 0.015	---
Pd	ug / g metal	< 0.027	---	< 0.045	---	Th	ug / g metal	< 0.015	---	< 0.009	---
Ag	ug / g metal	< 0.009	---	< 0.015	---	Total U	ug / g metal	1010000	50000	1010000	50000
						Total U	wt %	101	5	101	5

Notes: Elements highlighted in yellow were run in collision-cell mode to reduce polyatomic interferences. Ta is highlighted in blue, because, although detected, its exact concentration is uncertain (+/-50% est.) due to its instability in solution.

Stable isotope Analysis

Some of the fines from the cutting (aliquoting) operation were analyzed by stable isotope mass spectrometry for C, N, O, and S content, as well as C isotopic composition. The results are listed in Table 11. The carbon content of both samples is extremely high.

Table 11. Stable Isotope Results from Samples FSC-10-1-1 and FSC-10-1-2

Sample	ID	Wt. % C*	+/-	Wt. % N	+/-	Wt. % S	+/-	Wt. %O**	+/-	d13C (per mil)	+/-
A	FSC-10-1-2	0.170%	0.005%	<0.02%		<0.02%				-21.2	0.3
B	FSC-10-1-1	0.115%	0.007%	<0.02%		<0.02%		6.77%	0.29%	-21.3	0.3
*Wt. % C in U metal											
**All oxygen is assumed to have been derrived from oxidation during cutting, i.e. it was not in the original U metal sample											

The d13C values (-21.2 and -21.3 per mil) are consistent with C3 plants, coal or graphite. The fact the the values are the same within error, strongly suggests that the carbon came from the same source in both samples. This would indicate that they were likely made in the same facility, using the same materials. The different % C compositions would suggest that they are not two pieces of the same material, but were melted/cast separately.

Unfortunately, due to the nature of the sample used for stable isotope analysis, the measured O content is most likely due to surface oxidation and/or oxidation during the cutting process. Therefore, we cannot use it to assess the quality of the vacuum during casting.

Radiochemistry

Sub-sample C for sample B (FSC-10-1-1) and sub-sample B for sample A (FSC-10-1-2) were dissolved, relevant elemental fractions were separated and purified, and the resulting solutions analyzed by radioactive decay counting. Uranium Isotopic results are listed in Table 12. Plutonium isotopic results are listed in Table 13. Neptunium concentrations are listed in Table 14.

"Model Ages" as determined by radiochemistry and alpha spectrometry are shown in Table 15 ($^{234}U \rightarrow ^{230}Th$ system) and Table 16 ($^{241}Pu \rightarrow ^{241}Am$ system). These model ages estimate the time since last chemical purification of the parent nuclide from the daughter nuclide (assuming complete purification). Incomplete purification or impurity segregation during later processing will lead to ages that are higher than the true time since last chemical purification.

In addition, alpha spectroscopy was performed on the mass spectrometry aliquots for determination of ^{228}Th and ^{232}U. The concentrations of ^{228}Th and ^{232}U from this set of analyses are listed in Table 17. The $^{232}U/^{235}U$ ratios are listed in Table 18 and the model age, as determined by $^{232}U \rightarrow ^{228}Th$ are listed in Table 19.

Table 12. Uranium isotopic composition from Radiochemistry/Alpha Spectroscopy

		Atomic Ratios					
ITWG Sample ID	FSC Sample ID	232U/235U	Expanded Uncert. (k=2)	234U/235U	Expanded Uncert. (k=2)	238U/235U	Expanded Uncert. (k=2)
Sample A	FSC-10-1-2	1.15E-10	1.9E-11	1.060E-02	6.8E-04	4.6E-02	8.6E-02
Sample B	FSC-10-1-1	1.45E-10	2.1E-11	1.060E-02	6.5E-04	8.9E-02	8.2E-02

Table 13. Plutonium isotopic composition from Radiochemistry/Alpha Spectroscopy

		atomic ratios		ng/g U-metal	
	Sample ID	238Pu/239Pu	Expanded Uncertainty (k=2)	Total Pu	Expanded Uncertainty (k=2)
Sample A	FSC-10-1-2-C	4.657E-03	9.9E-05	6.77	0.16
Sample B	FSC-10-1-1-B	2.390E-03	9.3E-05	14.86	0.61

Table 14. Neptunium concentrations from Whole Solution Gamma Spectroscopy

		atomic ratio	
	Sample ID	237Np/238U	std. uncert.
Sample A	FSC-10-1-2-C	5.2E-06	1.1E-06
Sample B	FSC-10-1-1-B	3.78E-06	7.6E-07

Table 15. Age-dating from Radiochemistry & Alpha Spectroscopy using the $^{234}U \rightarrow ^{230}Th$ System

		atoms/g U-metal		atoms/g U-metal		atomic ratio	
	Sample ID	230Th	Expanded Uncertainty (k=2)	234U	Expanded Uncertainty (k=2)	230Th / 234U	Expanded Uncertainty (k=2)
Sample A	FSC-10-1-2-C	5.07E+14	4.8E+13	2.5587E+19	3.5E+16	0.0000198	0.0000019
Sample B	FSC-10-1-1-B	3.95E+14	4.6E+13	2.4915E+19	3.4E+16	0.0000159	0.0000018

Years before Reference Date: 2-Apr-10

	Sample ID	Model Age (years)	Expanded Uncertainty (years)	Model Date	Expanded Uncertainty (days)
Sample A	FSC-10-1-2-C	7.01	0.67	29-Mar-03	243
Sample B	FSC-10-1-1-B	5.62	0.65	21-Aug-04	239

Table 16. Age-dating from Radiochemistry & Alpha Spectroscopy using the $^{241}Pu \rightarrow ^{241}Am$ System

		ng/g U-metal		atoms/g U-metal		atoms/g U-metal		atomic ratio	
	Sample ID	241Am	Expanded Uncertainty (k=2)	241Am	Expanded Uncertainty (k=2)	241Pu	std. uncert.	241Am / 241Pu	std. uncert.
Sample A	FSC-10-1-2-C	0.0037	0.0004	9.3E+09	1.0E+09	1.036E+10	2.3E+08	9.02E-01	0.10
Sample B	FSC-10-1-1-B	0.0084	0.0010	2.1E+10	2.6E+09	1.922E+10	4.0E+08	1.09E+00	0.14

Years before Reference Date: 25-Mar-10

	Sample ID	Model Age (years)	Expanded Uncertainty (years)	Model Date	Expanded Uncertainty (days)
Sample A	FSC-10-1-2-C	12.3	1.3	9-Dec-97	490
Sample B	FSC-10-1-1-B	15.3	1.9	30-Nov-94	686

Table 17. ^{228}Th and ^{232}U Concentrations from Alpha Spectroscopy on the ICP-MS fraction

		atoms/g U-metal		atoms/g U-metal	
	Sample ID	**228Th**	Expanded Uncert. (k=2)	**232U**	Expanded Uncert. (k=2)
Sample A	FSC-10-1-2-C	9.05E+09	9.5E+08	4.4E+11	1.4E+11
Sample B	FSC-10-1-1-B	9.4E+09	1.2E+09	5.0E+11	1.4E+11

Table 18. ^{228Th}/ ^{232}U Ratios from Alpha Spectroscopy on the ICP-MS fraction

	Sample ID	232U/235U	Expanded Uncert. (k=2)
Sample A	FSC-10-1-2-C	1.85E-10	5.7E-11
Sample B	FSC-10-1-1-B	2.16E-10	5.6E-11

Table 19. ^{232}U →^{228}Th Model Ages from Alpha Spectroscopy on the ICP-MS fraction

Reference Date: 10-April-2010			
		228Th -- 232U Model Age	
	Sample ID	Model age (years)	Expanded Uncert. (k=2)
Sample A	FSC-10-1-2-C	3.7	2.6
Sample B	FSC-10-1-1-B	3.0	1.6

SEM/EDS/EMPA Characterization of Polished Surfaces

Samples were cut for metallurgical analysis along orthogonal axes, embedded in epoxy and polished using carborundum-impregnated discs. Final polishing was performed with 3- and 1-micron diamond paste. Mineral oil was used as the lubricant to minimize corrosion. Samples were examined in a JEOL JSM-7401F SEM equipped with an Oxford Inca X-max 80 EDS. The majority of images, and EDS analyses, were collected at 10 keV using backscattered electrons. Quantitative analyses of uranium carbides were performed with a JEOL JXA-8200 electron microprobe.

Both samples contain similar populations of small inclusions. Uranium carbide (U-C) is the most abundant, followed by uranium phosphide (U-P-C), uranium boron-carbide (U-B-C), Fe-Ni-U carbide and (possibly) SiC. Insofar as carborundum was used to prepare the samples, we cannot exclude the possibility that some of the SiC is a contaminant. Quantifying the chemical composition of the inclusions based on SEM/EDS analyses was not possible due to the intense x-ray emission corresponding to the U Na transition. The U Na peak fully overlaps the C Ka peak, making it very difficult to determine accurately the C content of any inclusion containing U as a major constitutent. Instead, we preformed quantitative analyses of 10 larger U-C inclusions using wavelength dispersive analysis with the electron microprobe. The results of these analyses (table 20) indicate the larger, orthorhombic U-C inclusions are uranium monocarbide (UC).

Table 20. Uranium carbide compositions (uncertainties are 1-sigma)

No.	C (wt%)	U (wt%)	Total	C (atom%)	U (atom%)
1	4.57	96.05	100.62	48.50	51.49
2	4.78	96.13	100.91	49.62	50.37
3	4.73	95.83	100.56	49.44	50.55
4	5.18	95.97	101.15	51.69	48.30
5	4.29	94.63	98.92	48.33	50.61
6	4.57	95.00	99.57	48.82	51.17
7	4.21	95.35	99.56	46.64	53.35
8	4.80	96.53	101.33	49.61	50.38
9	4.82	96.42	101.24	49.76	50.23
10	4.70	95.72	100.42	49.41	50.51
Average	***4.66±0.29***	***95.77±0.64***	***100.43±0.87***	***49.2±1.4***	***50.7±1.3***

The different types of inclusions exhibit different characteristic morphologies, making it possible, in many cases, to identify an inclusion based solely on appearance. Images of the inclusions illustrating the characteristic shapes are shown in Figures 35-37.

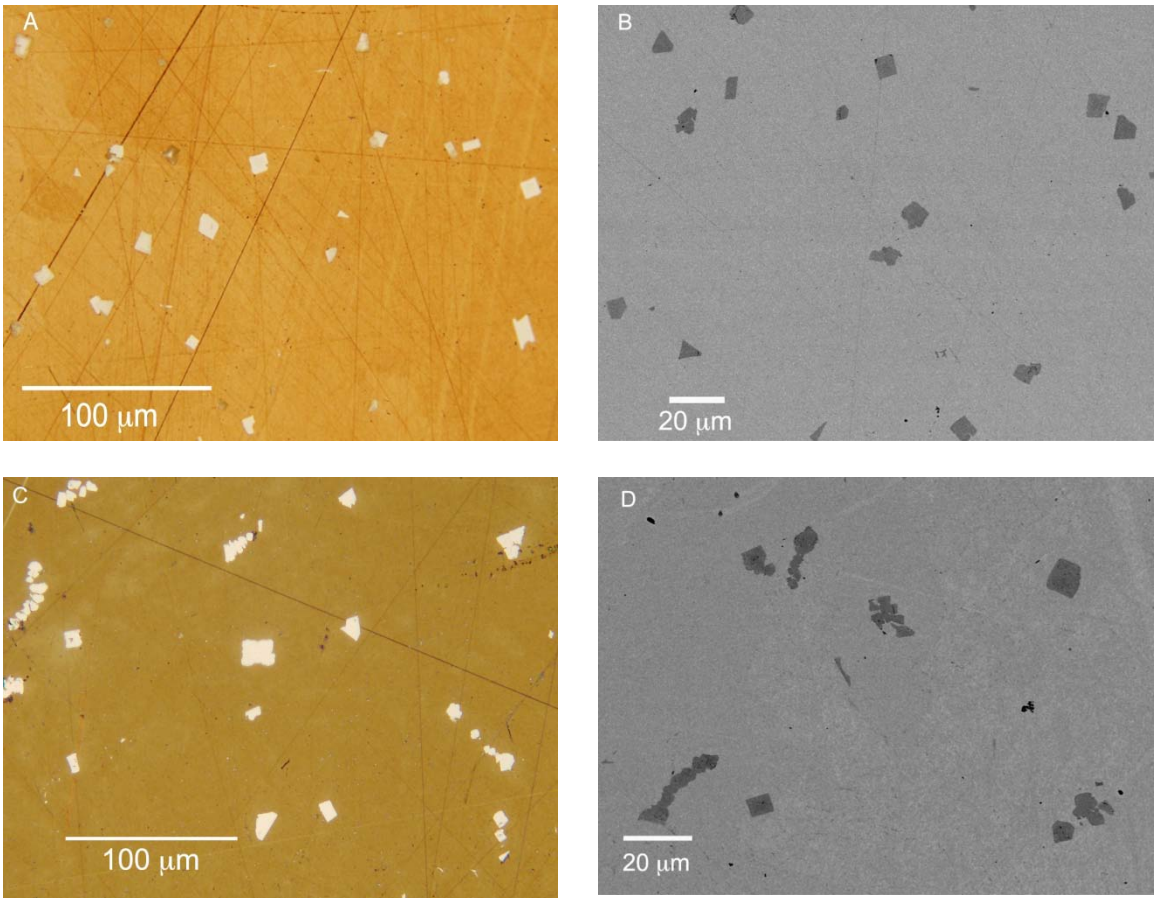

Figure 35. Paired optical (lefthand column) and SEM backscattered electron (righthand column) photomicrographs of inclusions in the U-metal samples. Images A – D are relatively low magnification images (~300 to 500x) showing arrays of UC inclusions. The UC inclusions have typical sizes of 5 – 10 mm. Images A & B show sample 10-1-1-A, while images C – D show sample 10-1-2-A.

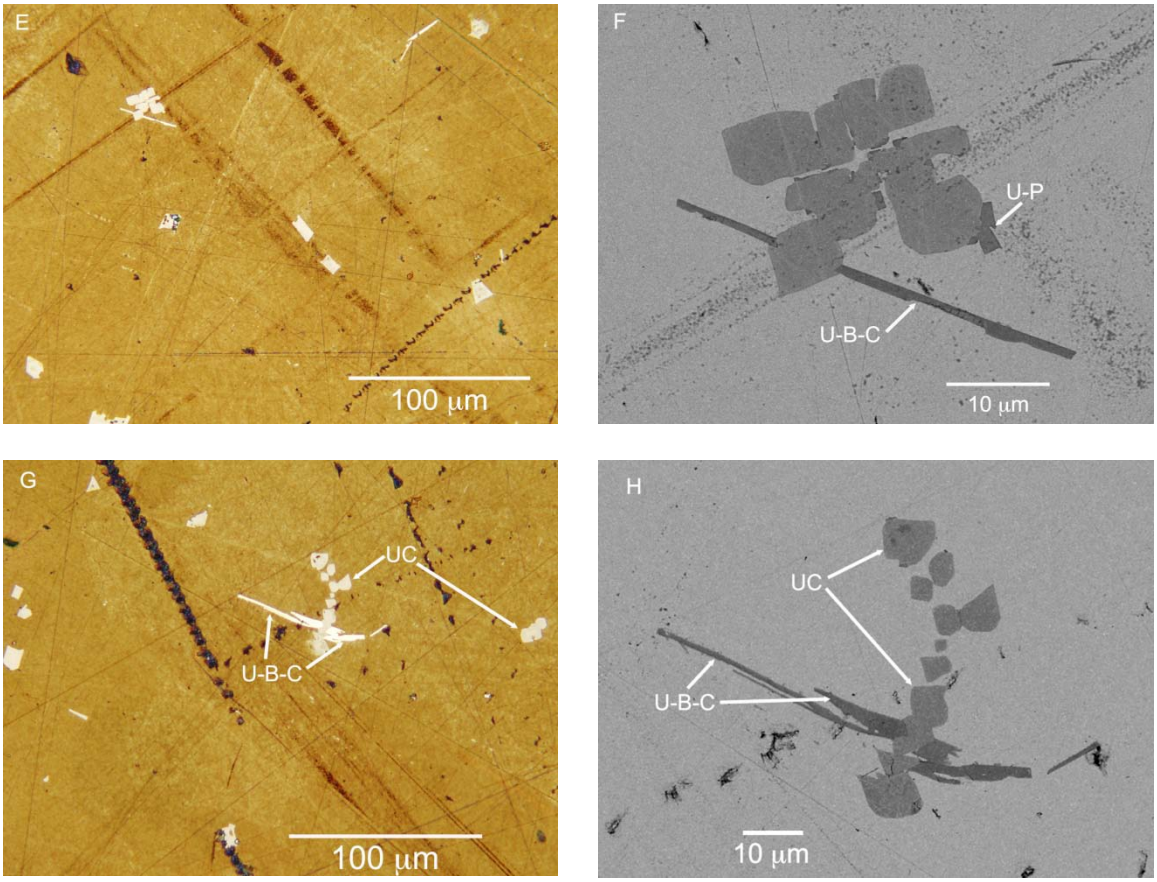

Figure 36. Paired optical (lefthand column) and SEM backscattered electron (righthand column) photomicrographs of inclusions in the U-metal samples. Images E & F show UC inclusions intergrown with elongate U-B-C inclusions; image F is a close-up view of the assemblage visible in the upper lefthand quadrant of image E. The U-B-C inclusions exhibit a characteristic elongate shape with typical width ratios of 5 to 20. Also visible in image F are several U-P inclusions attached to larger UC inclusions. Images G & H show elongate U-B-C inclusions cross-cutting a string of orthorhombic UC inclusions. Images E–H show sample 10-1-2-A.

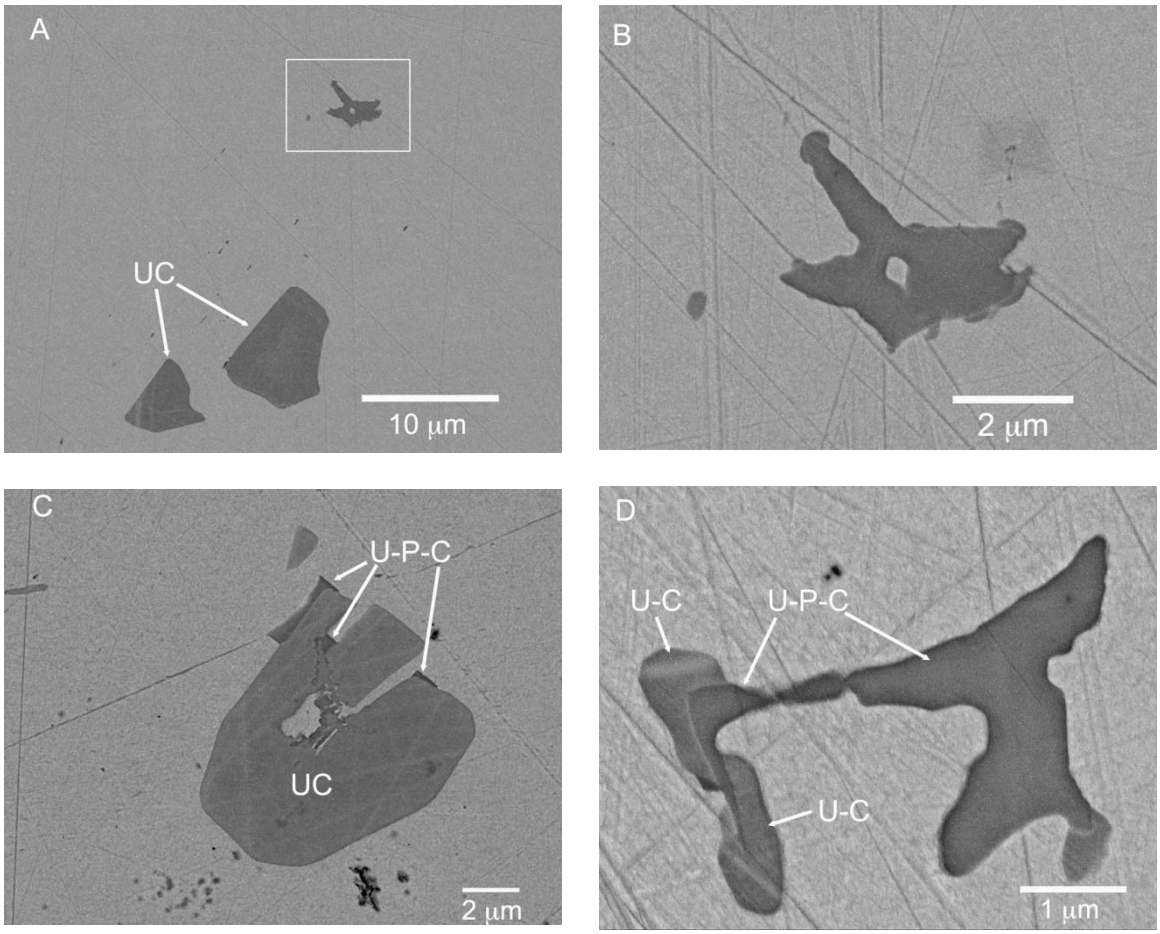

Figure 37. SEM backscattered electron images of U-P-C inclusions in U-metal. Several different types of occurrences are observed. Images A and B (sample 10-1-1) show an isolated U-P-C inclusion; image B is a close up of the area contained in the rectangle in image A. The bright area in the center of the U-P-C inclusion is U-metal. Image C (sample 10-1-2) shows U-P-C attached to the exterior surfaces of a larger UC inclusion. Image D (sample 10-1-1) shows an inclusion composed of intergrown U-P-C and U-C. The irregular shapes shown in images B and D are characteristic of U-P-C inclusions.

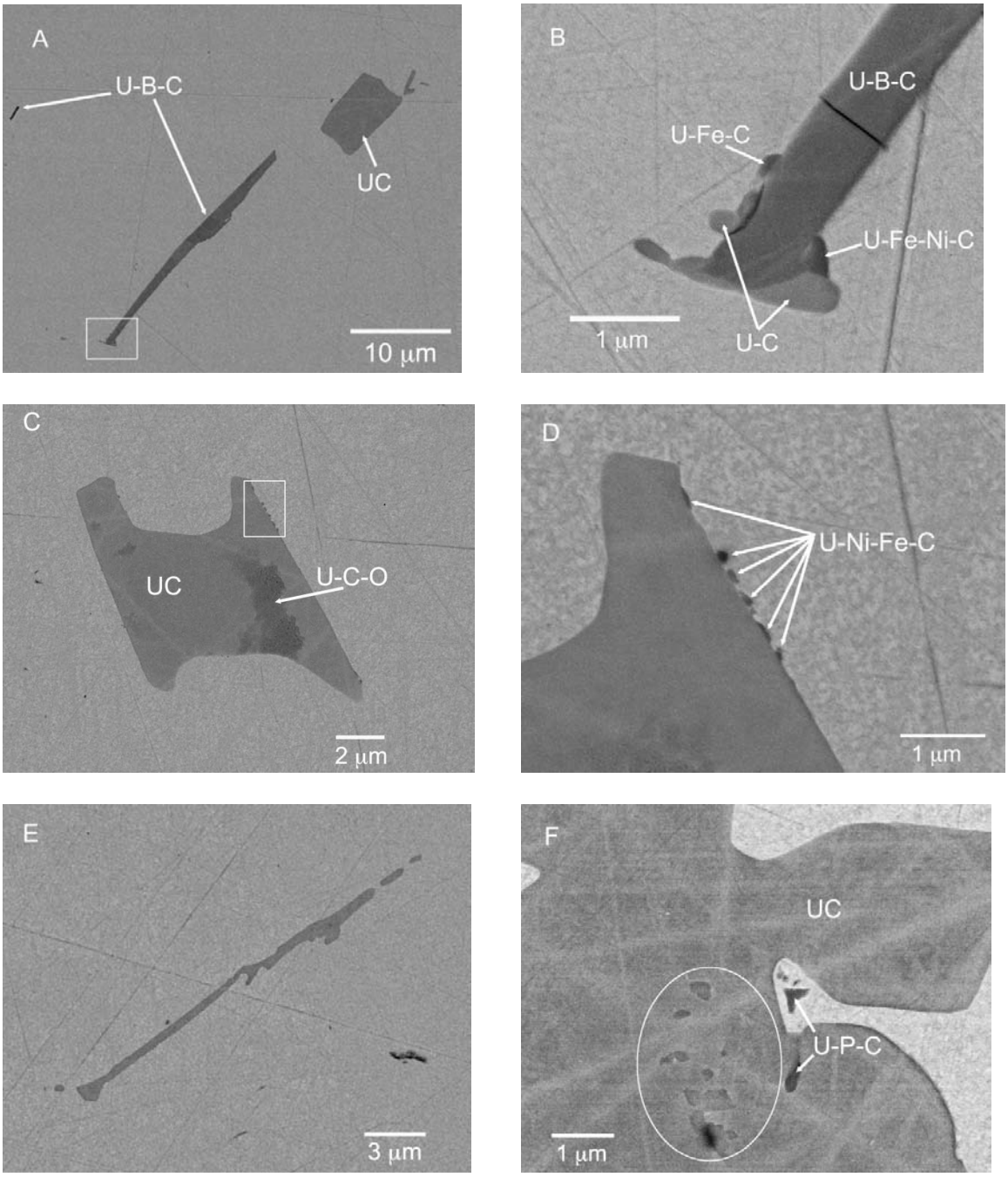

Figure 38. SEM backscattered electron images of rare inclusions in the U-metal samples. Images A shows two elongate U-B-C inclusions in sample 10-1-1; the boxed area is highlighted in image B. Image B shows complex intergrowth of several different types of carbide inclusions: U-B-C, U-C (the stoichiometry was not determined), U-Fe-Ni-C and U-Fe-C; the latter two inclusions also contain ~1-2 wt.% Si. Images C and D show a UC inclusion in sample 10-1-2 decorated with numerous sub-micron size U-Fe-Ni-C inclusions, some of which contain up to 1 wt. % Si. Image E shows a very elongate U-C inclusion with irregular borders; despite its unusual shape, the inclusion appears to be UC. Image F (sample10-1-2) shows a UC inclusion containing submicron size inclusions of U-P-C and an unusual S-bearing carbide phase (contained within the ellipse) in which S appears to substitute for P.

To date, we have not been able to successfully electropolish the cross-sections to reveal the grain structure of the uranium. We believe that these parts were cast, but the grain structure would provide convincing evidence of the method of manufacture.

Mass Spectrometry & Radiochemistry Comparison

Mass spectrometry (MS) and radiochemistry (RC) measurements of the same material characteristic are compared in Table 20, except for U232/U235, which was measured by alpha spectrometry on the mass spec aliquot in one case and whole solution gamma spectroscopy on the radiochemistry aliquot in the other case. Radiochemistry/alpha spectrometry was also performed on the radiochemistry aliquote, but detection limits higher than the values reported in Table 20 were obtained.

All measured values agree within analytical uncertainty, except for the Am-241 concentration (which then affects the Pu241-Am241 age). Since the disagreement is similar between the analyses of Sample A and Sample B (16-17 %), it suggests a small systematic error.

The measured values for U232/U235 lie close to analytical uncertainty, again the disagreement being similar between the analyses of Sample A and Sample B. Therefore, the differences between the two techniques also deserves closer scrutiny.

Table 21. Comparison of Mass Spectrometry (MS) and Radiochemistry (RC) Measurements
Note: Agreement here is defined as:
(MS Value-RC Value)/(MS Exp. Unc.+RC Exp. Unc.) expressed as a percentage.

			MS		RC		Agree
Measurement	**Sample**	**Units**	**Value**	**Exp. Unc.**		**Exp. Unc.**	
U234/U235	A		1.07944E-02	4.3E-06	1.060E-02	6.8E-04	28%
	B		1.06842E-02	4.3E-06	1.060E-02	6.5E-04	13%
U238/U235	A		6.0517E-02	6.6E-05	4.6E-02	8.7E-02	17%
	B		7.7680E-02	8.4E-05	8.9E-02	8.2E-02	-14%
Pu Concentration	A	ng/g U	7.04	0.24	6.77	0.16	68%
	B		14.10	0.48	14.86	0.61	-70%
Np237/U235	A		4.72E-06	1.7E-07	5.2E-06	1.1E-06	-35%
	B		3.73E-06	1.3E-07	3.78E-06	7.6E-07	-6%
U234-Th230 Age	A	years	6.861	0.041	7.02	0.67	-22%
	B		6.041	0.036	5.62	0.65	62%
Pu241-Am241 Age	A	years	14.35	0.33	12.3	1.3	126%
	B		17.46	0.37	15.3	1.9	95%
Th230 Concentrati	A	atoms/g	4.962E+14	1.2E+12	5.07E+14	4.8E+13	-22%
	B		4.254E+14	1.0E+12	3.95E+14	4.6E+13	65%
Am241 Concentrat	A	atoms/g	1.0920E+10	5.4E+07	9.3E+09	1.0E+09	147%
	B		2.433E+10	1.2E+08	2.1E+10	2.6E+09	123%
			MS-Alpha		**Whole Solution Gamma**		
Measurement	**Sample**	**Units**	**Value**	**Exp. Unc.**		**Exp. Unc.**	
U232/U235	A		1.85E-10	5.7E-11	1.15E-10	1.9E-11	91.86%
	B		2.16E-10	5.6E-11	1.45E-10	2.1E-11	92.45%

Age Dating Comparison

Table 22. Comparison of Model Ages from Different Isotopic Systems

			MS		RC		Agree
Measurement	**Sample**	**Units**	**Value**	**Exp. Unc.**		**Exp. Unc.**	
U234-Th230 Age	A	years	6.861	0.041	7.02	0.67	-22%
	B		6.041	0.036	5.62	0.65	62%
U235-Pa231 Age	A	years	33.73	0.36			
	B		35.77	0.37			
U232-Th228 Age	A	years	3.7	2.6			
	B		3.0	1.6			
Pu241-Am241 Ag	A	years	10.21	0.26	12.3	1.3	-134%
	B		12.66	0.30	15.3	1.9	-120%

The first three model ages (234U→230Th, 235U→231Pa, 232U→228Th) theoretically reflect the age of the uranium (time since last chemical separation of parent and daughter nuclides). The last model age (241Pu→241Am) theoretically reflects the age of the plutonium. If the U and Pu were associated during the chemical purification, then we would expect those ages to agree. On the other hand, if the Pu became associated afterwards, e.g., through contamination, then we would not expect those ages to agree.
At first, the disagreement between the 3 U ages is somewhat troubling. However, the agreement between mass spectrometry and radiochemistry values on two separate aliquots of both samples suggests that our original assumption is not valid. In order for the model age to be the true age, two assumptions must hold true. First, the uranium must be completely purified of its daughter nuclides at a single point in time. In addition, for all 3 U ages to agree, the uranium must be completely purified of all 3 daughter nuclides (230Th, 231Pa, and 228Th). Second, after purification, there must be no process that leads to segregation of the parent and daughter nuclides.

As we will show in the technical interpretation section to follow, there is evidence that these samples were prepared by mixing of two different lots of uranium. There has been substantial empirical evidence that the uranium casting process can lead to segregation of the daughter products to the top of the melt, depending on the rate of cooling. We would also expect that this segregation process might vary from element to element. Therefore, ages from U metal must be treated with caution.

One still might expect agreement between the two U-Th ages (234U→230Th, 232U→228Th). However, the 232U/228Th system reaches secular equilibrium quite quickly. Therefore, if one of the components of the U mixture were older than the length of time needed to reach secular equilibrium, we might expect the 228Th content to be lower than that expected from the 234U→230Th age.

Technical Interpretation

Note: Technical interpretations are technical judgments based upon current results.

All uranium isotopic analyses indicate that both samples are weapons-usable, highly enriched uranium. Therefore, both seizures indicate that the statutes of the country of Texmex regarding the transport of uranium materials have been violated (>1 gram, >1% enriched in U235).

The $^{234}U/^{235}U$ ratio indicates likely isotopic enrichment via either a gaseous diffusion or centrifuge process, rather than electromagnetic or laser isotope separation.

The presence of ^{232}U, ^{233}U, ^{236}U, and ^{237}Np indicates that some of the enrichment feed stock had been irradiated in a reactor, such recycling of irradiated uranium is more consistent with known gaseous diffusion plant operations than centrifuge operations.

Isotopic analysis by multicollector inductively coupled plasma-mass spectrometry (MC-ICP-MS) indicates that the two samples (Sample A, Sample B) have isotopic compositions that differ outside analytical uncertainty (k=2). The model ages of the two samples (apparent time since last chemical separation of parent and daughter nuclides) also differ outside analytical uncertainty (k=2). These results would indicate that, even with all of the other similarities between the two samples, the two questioned samples originate from different source materials.

The enrichment values for both samples are similar to, but different than, 93% enrichment values found in several countries, e.g., the United States.

In our experience the $^{238}U/^{235}U$ ratio and $^{234}U/^{235}U$ ratio are fairly constant in US HEU production (~1 % variability). If you plot the values from the ITWG Sample A and Sample B on a 3-isotope plot ($^{238}U/^{235}U$ ratio versus $^{234}U/^{235}U$ ratio), along with typical values for US HEU (93.15% U-235), the three values like along a straight line, suggesting that the two ITWG samples may have been made by down-blending US HEU slightly. We found that the best fit for the material used to down-blend the HEU was 70% enriched US HEU. All four points lie along a straight line (R^2=0.9998). For comparison, NBL U650 (65% U-235) and U750 (75% U-235), also produced from material from the US diffusion enrichment system, are shown on Figure 38 to lie well off the mixing line. This suggests that Sample A (FSC-10-1-2) is a blend of approximately 1% of 70% enriched material and 99% of US HEU (93.15% enriched) and Sample B (FSC-10-1-1) is a blend of approximately 5.7% of 70% enriched material and 94.3% of US HEU (93.15%).

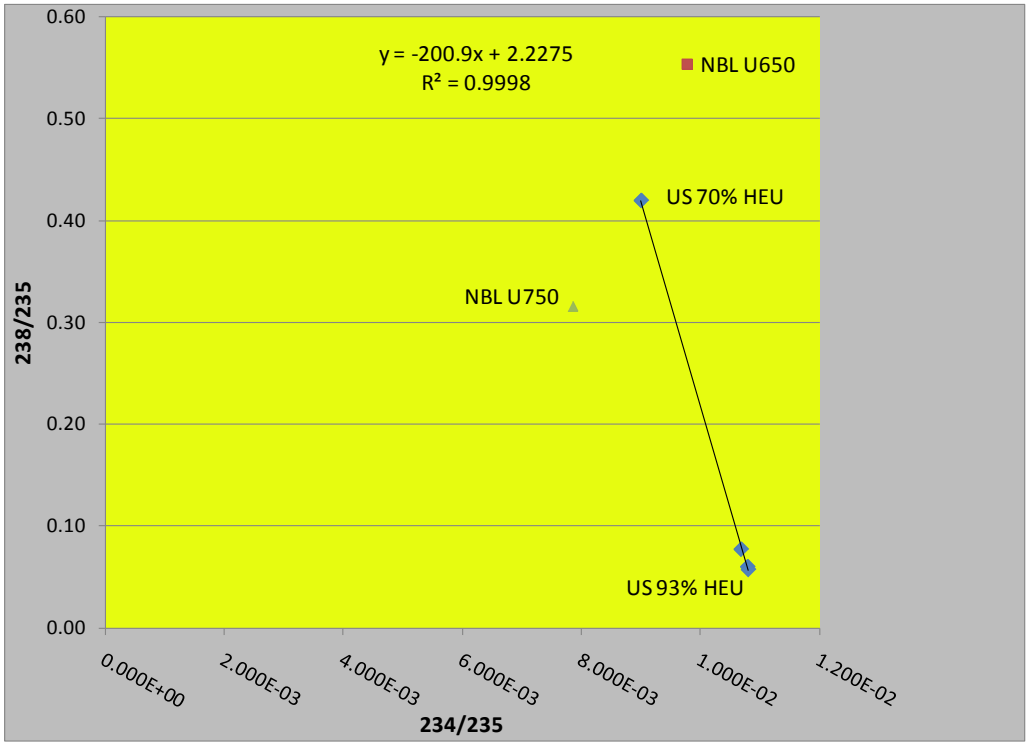

Figure 39. 3-isotope Plot of ITWG Samples versus Typical US HEU Compositions

As noted previously, the model ages of the two samples (time since last chemical separation of parent and daughter nuclides) also differ outside analytical uncertainty (k=2). If these two samples were created by blending two materials of different ages, then, in the best case, the resulting material would have a model age that is a weighted average of the ages of the starting materials. However, as described in the age-dating section, there can be segregation of the daughter nuclides from the parent nuclides during casting. So, the difference between the two ages must also be treated with caution. In order to properly compare the ages of the two materials, we would have to know that they were cast in the same way (mass, cooling time, etc.).

Uranium parts are typically cast using graphite molds with coatings of erbia, zirconia, or yttria. The high level of carbon in these samples likely originates from the graphite molds –the molds used for this casting, as well as previous castings of the component materials. In fact, the extremely large amount of carbon in these samples suggests a significant amount of recycling.

We also see residue from the erbia and zirconia mold coatings, which must be from previous, separate castings, since erbia and zirconia are typically not used in combination. We do not see any evidence of the use of an yttria mold coating.

The presence of uranium phosphide inclusions in the uranium metal is somewhat unusual. We did find reference to uranium phosphide inclusions in uranium derby metal (initial metal converted from UF_4) of high phosphorus content. However, the paper did not elaborate on the nature or origini of the high phosphorus content.

In addition, the geometry of these samples suggests that they are pieces from a larger part of annular cross-section. Annular castings are typical storage configurations for HEU. This implies that the original material may have been part of a location that stores significant amounts of HEU.

The surfaces of the interdicted samples showed evidence of the as-cast surface, as well as two different types of machining (different pattern of grooves on the top/bottom versus the sides). The striations on the top/bottom (flat sides) are 15/mm. They may occur either from direct machining of the metal or machining of the mold, which then leaves its imprint on the metal during casting. The lower frequency striations along the long sides were probably produced during cutting of these pieces from the master object. The ends of the pieces are probaby "as cast."

In summary:

The sum of these observations suggests that these samples are from a large nuclear weapons state. This state probably uses gaseous diffusion for enrichment and includes recycled uranium in the production cycle.

Based upon the geometry o the initial object, as extrapolated from the geometry of the interdicted sample, this materialwas probably diverted from a facility used to storing large amounts of highly enriched uranium. This facility probably also includes the facilities for casting, machining, and cutting uranium parts.

However, the purpose of blending down the original 93% enrichment value using 70% enriched material is unknown. This particular material, though, is not highly refined metal and was likely not intended for weapons use without further processing or refinement.

Application of ITWG Guideline on Graded Comparison

We first applied the Provisional ITWG Guideline on Graded Comparison to the issue of whether or not the laws of the country of TexMex were violated. For this, we modified the "Univariate (one variable) determination/Determination above vs. below a legal limit" to a bivariate determination, since the laws of TexMex require two conditions to be satisfied (mass & enrichment) to break their law. From this analysis, we determined that both conditions were "conclusive positive above" the threshold.

Table 23. Application of ITWG Guideline to Legal Limits of TexMex

Bivariate Above/Below Legal Statute						
Measurand	**Sample**	**Value**	**Unit**	**Exp. Unc. (k=3)**	**Legal Limit**	**Value>Legal+Exp. Unc.**
U235 Content	A	92.98%		0.0128%	1%	YES
	B	91.51%		0.0141%	1%	YES
Mass	A	5.0640	grams	0.0002	1	YES
	B	5.6196	grams	0.0002	1	YES
Result:	Conclusive positive above					

We then applied the Provisional ITWG Guideline on Graded Comparison to the issue of whether or not the two samples were similar or dissimilar. For this, we used the "Multivariate (multiple characteristics) –a joint similarity/dissimilarity determination of characteristics." We determined a lot of characteristics as shown in the table below. Essentially, there were equal numbers of characteristics that were similar (either conclusive or suggestive) and dissimilar (either conclusive or suggestive). This would lead to an "inconclusive" determination without weighting (as allowed by the guideline).

The basic problem is that the parts are similar in some aspects (basic geometry, some of the dimensions, many of the trace elemental concentrations), but the source material is clearly different (isotopics, model ages). Therefore, if one were interested in the samples' similarity/dissimilarity regarding source of the material, one should weight characteristics like isotopic composition and age higher than other characteristics. On the other hand, if one were more interested in whether the samples had been prepared by a similar process (but not the same material), then one should weight characteristics like metallurgical evaluations, trace elemental compositions, etc., more highly than other characteristics.

Table 24. Application of ITWG Guideline to Similarity/Dissimilarity of Sample A & B

Measurand	Type	Unit	Sigmas	Result
Mass	Quantitative	grams	2778	CONCLUSIVE DISSIMILAR
Length	Quantitative	mm	2.5	SUGGESTIVE SIMILAR
Width, low	Quantitative	mm	9.5	CONCLUSIVE DISSIMILAR
Width, high	Quantitative	mm	8.5	CONCLUSIVE DISSIMILAR
Thickness	Quantitative	mm	3.5	CONCLUSIVE DISSIMILAR
U233	Quantitative	%	2.3	SUGGESTIVE SIMILAR
U234	Quantitative	%	64	CONCLUSIVE DISSIMILAR
U235	Quantitative	%	165	CONCLUSIVE DISSIMILAR
U236	Quantitative	%	35	CONCLUSIVE DISSIMILAR
U238	Quantitative	%	215	CONCLUSIVE DISSIMILAR
Pu240/Pu239	Quantitative		7.6	CONCLUSIVE DISSIMILAR
Pu241/Pu239	Quantitative		8.8	CONCLUSIVE DISSIMILAR
Pu242/Pu239	Quantitative		9.2	CONCLUSIVE DISSIMILAR
Total Pu	Quantitative	ng/g	20	CONCLUSIVE DISSIMILAR
Np237	Quantitative	%	6.6	CONCLUSIVE DISSIMILAR
U234 Age	Quantitative	years	21	CONCLUSIVE DISSIMILAR
Pu241 Age	Quantitative	years	8.8	CONCLUSIVE DISSIMILAR
U235 Age	Quantitative	years	5.6	CONCLUSIVE DISSIMILAR
U Assay	Quantitative	g U/g sample	0.1	CONCLUSIVE SIMILAR
Al Impurity	Quantitative	ug/g	0.6	SUGGESTIVE SIMILAR
V Impurity	Quantitative	ug/g	0.3	CONCLUSIVE SIMILAR
Cr Impurity	Quantitative	ug/g	0.8	SUGGESTIVE SIMILAR
Mn Impurity	Quantitative	ug/g	1.0	SUGGESTIVE SIMILAR
Fe Impurity	Quantitative	ug/g	2.2	SUGGESTIVE SIMILAR
Co Impuirty	Quantitative	ug/g	0.1	CONCLUSIVE SIMILAR
Ni Impurity	Quantitative	ug/g	1.3	SUGGESTIVE SIMILAR
Cu Impurity	Quantitative	ug/g	0.4	CONCLUSIVE SIMILAR
Zr Impurity	Quantitative	ug/g	10	CONCLUSIVE DISSIMILAR
Mo Impurity	Quantitative	ug/g	0.2	CONCLUSIVE SIMILAR
Er Impurity	Quantitative	ug/g	6.6	CONCLUSIVE DISSIMILAR
W Impurity	Quantitative	ug/g	0.9	SUGGESTIVE SIMILAR
Re Impurity	Quantitative	ug/g	36	CONCLUSIVE DISSIMILAR
Ir Impurity	Quantitative	ug/g	7.2	CONCLUSIVE DISSIMILAR
Pt Impurity	Quantitative	ug/g	0.1	CONCLUSIVE SIMILAR
Wt% C	Quantitative	%	9.2	CONCLUSIVE DISSIMILAR
Delta Carbon	Quantitative	‰	0.3	CONCLUSIVE SIMILAR
U232/U235	Quantitative		0.5	SUGGESTIVE SIMILAR
Pu238/Pu239	Quantitative		24	CONCLUSIVE DISSIMILAR
U232 Age	Quantitative	years	0.3	CONCLUSIVE SIMILAR
Shape	Qualitative			CONCLUSIVE SIMILAR
Inclusions	Qualitative			CONCLUSIVE SIMILAR
IR-Vis Absorption	Qualitative			CONCLUSIVE SIMILAR
Organic Analysis	Qualitative			SUGGESTIVE SIMILAR
Optical Microscopy-General	Qualitative			CONCLUSIVE SIMILAR
Written Number	Qualitative			CONCLUSIVE SIMILAR
SEM Analysis-General	Qualitative			CONCLUSIVE SIMILAR

Table 25. Summary of Application of ITWG Guideline to Similarity/Dissimilarity of Sample A & B

CONCLUSIVE DISSIMILAR	22
SUGGESTIVE DISSIMILAR	0
INCONCLUSIVE	0
SUGGESTIVE SIMILAR	10
CONCLUSIVE SIMILAR	14
TOTAL	46
Result:	INCONCLUSIVE

Alternative Similarity Calculation

As a comparison to the method proposed by the current draft ITWG guideline, Pat Grant of the LLNL Forensic Science Center provided the following alternative approach.

Three subsets of the final RR3 data were compared. They were the MC-ICP-MS values (n = 11), the ICP-MS values (n = 15), and combined SIMS (n = 1) and radiochemistry (n = 5) values. The computations were statistical similarity comparisons between 10-1-1 *vs* 10-1-2, weighted instrumentally by the reported uncertainties.

Not all of the isotopic measurements were selected, as input data should be independent and uncorrelated as far as possible. Therefore, the daughter species for the chronometry studies were specifically excluded. The same tactic should perhaps have been performed for the trace-element data as well, because (e.g.) other components of steel might very well be correlated with Fe. But Pat had no satisfactory protocol for data rejection that could be defended, so he used all of the trace element impurity measurements above background.

The Discrepancy Index is the square of the weighted Euclidean distance in n-parameter space. All three subsets of measurements gave a quantitative 0% similarity correlation between the two RR3 specimens. (Pat was going to combine all of the data for an n = 32 run had there been more tangible results, but it would be of no significance for this evaluation.)

Thus, contrary to the "inconclusive" result of Table 23, statistical analyses of all of the quantitative measurements made of the nuclear "source-term" materials are unambiguous for a conclusion of "no correlation." This is just the opposite determination derived from forensic assessments of surficial "route" signatures, however.

Table 26. Application of Discrepancy Index to Similarity/Dissimilarity of Sample A & B

COMMENT: ITWG RR3 MC-ICP-MS data; 10-1-1 vs 10-1-2; k=2 errors

SIMILARITY COMPARISON (Parker; upper, 1-sided test)

	q_i	Δq_i	Δq_i%	k_i	Δk_i	Δk_i%	d_i	Δd_i	f_i^2
233	4.310E-05	4.400E-06		3.290E-05	4.400E-06		0.00	6.223E-06	2.687E+00
234	9.777E-01	4.100E-04		1.004E+00	4.000E-04		-0.03	5.728E-04	2.064E+03
235	9.151E+01	9.400E-03		9.298E+01	8.500E-03		-1.48	1.267E-02	1.355E+04
236	4.062E-01	5.900E-04		3.860E-01	5.600E-04		0.02	8.134E-04	6.173E+02
238	7.108E+00	7.700E-03		5.627E+00	6.100E-03		1.48	9.823E-03	2.274E+04
240/9	6.238E-02	4.300E-04		6.574E-02	4.500E-04		0.00	6.224E-04	2.914E+01
241/9	5.560E-04	1.100E-05		6.620E-04	1.300E-05		0.00	1.703E-05	3.874E+01
242/9	1.086E-03	2.500E-05		1.375E-03	3.800E-05		0.00	4.549E-05	4.037E+01
[94k]	1.410E-05	4.800E-07		7.040E-06	2.400E-07		0.00	5.367E-07	1.731E+02
[93k]	3.420E-06	1.200E-07		4.410E-06	1.500E-07		0.00	1.921E-07	2.656E+01
[92k]	9.955E-01	2.500E-03		9.957E-01	2.500E-03		0.00	3.536E-03	3.200E-03
n =	11						0.00		3.928E+04

$\sum d_i$ = 0.00 **C =** 3.928E+04 = Discrepancy Index

Similarity Match C < C_0 for ε < **1.0 %** **(ε = 0 %)**

similarity.xls

Table 26 (cont.). Application of Discrepancy Index to Similarity/Dissimilarity of Sample A & B

COMMENT:		ITWG RR3 ICP-MS data; 10-1-1 vs 10-1-2; k=2 errors								
SIMILARITY COMPARISON (Parker; upper, 1-sided test)										
		q_i	Δq_i	Δq_i%	k_i	Δk_i	Δk_i%	d_i	Δd_i	f_i^2
	Al	2.730E+01	6.500E+00		2.310E+01	7.000E+00		4.20	9.552E+00	1.933E-01
	V	1.170E+00	6.000E-01		9.900E-01	6.000E-01		0.18	8.485E-01	4.500E-02
	Cr	2.280E+01	2.800E+00		2.050E+01	3.200E+00		2.30	4.252E+00	2.926E-01
	Mn	9.200E+00	9.000E-01		8.160E+00	1.100E+00		1.04	1.421E+00	5.354E-01
	Fe	9.900E+01	6.000E+00		8.800E+01	4.000E+00		11.00	7.211E+00	2.327E+00
	Co	9.900E-01	2.000E-01		9.800E-01	2.000E-01		0.01	2.828E-01	1.250E-03
	Ni	6.120E+01	3.100E+00		6.600E+01	4.300E+00		-4.80	5.301E+00	8.199E-01
	Cu	1.310E+01	1.400E+00		1.250E+01	1.600E+00		0.60	2.126E+00	7.965E-02
	Zr	1.045E+01	5.000E-01		5.800E+00	4.000E-01		4.65	6.403E-01	5.274E+01
	Mo	5.050E+01	1.400E+00		5.090E+01	1.800E+00		-0.40	2.280E+00	3.077E-02
	Er	4.500E-01	4.000E-02		2.200E-01	3.000E-02		0.23	5.000E-02	2.116E+01
	W	3.470E+01	5.000E-01		3.420E+01	6.000E-01		0.50	7.810E-01	4.098E-01
	Re	1.190E+00	1.000E-01		1.750E+01	8.000E-01		-16.31	8.062E-01	4.093E+02
	Ir	3.500E-01	3.000E-02		1.700E-01	2.000E-02		0.18	3.606E-02	2.492E+01
	Pt	4.300E-01	1.000E-01		4.200E-01	1.000E-01		0.01	1.414E-01	5.000E-03
	n =	15						3.39		5.128E+02
		$\sum d_i$ =	3.39		C =	5.128E+02	=	Discrepancy Index		
		Similarity Match C < C_0 for ε <			1.0 %		(ε =	0 %)		

similarity.xls

Table 26 (cont.). Application of Discrepancy Index to Similarity/Dissimilarity of Sample A & B

COMMENT:		ITWG RR3 SIMS & Radiochem. data; 10-1-1 vs 10-1-2; k=2 errors								
SIMILARITY COMPARISON (Parker; upper, 1-sided test)										
		q_i	Δq_i	Δq_i%	k_i	Δk_i	Δk_i%	d_i	Δd_i	f_i^2
	C	1.150E-01	7.000E-03		1.700E-01	5.000E-03		-0.06	8.602E-03	4.088E+01
92k	232/5	1.450E-10	2.080E-11		1.150E-10	1.920E-11		0.00	2.831E-11	1.123E+00
92k	234/5	1.060E-02	6.460E-04		1.060E-02	6.790E-04		0.00	9.372E-04	0.000E+00
92k	238/5	8.900E-02	8.200E-02		4.600E-02	8.650E-02		0.04	1.192E-01	1.302E-01
94k	238/9	2.390E-03	9.280E-05		4.660E-03	9.900E-05		0.00	1.357E-04	2.799E+02
	[94k]	1.486E-08	6.100E-10		6.770E-09	1.600E-10		0.00	6.306E-10	1.646E+02
	n =	6						-0.01		4.866E+02
		$\sum d_i$ =	-0.01		C =	4.866E+02	=	Discrepancy Index		
		Similarity Match C < C_0 for ε <			1.0 %		(ε =	0 %)		

similarity.xls